



ORIGINAL ARTICLE



# Assessing the Impact of Long-Term Drought on Agriculture in Bangladesh Using Multisource Remote Sensing Data

Nur Hussain<sup>1</sup> · Md Saifuzzaman<sup>2</sup> · Mohd. Shamsul Alam<sup>3</sup> · Md Shamim Ahamed<sup>4</sup>

Received: 13 February 2025 / Revised: 6 July 2025 / Accepted: 2 August 2025  
© King Abdulaziz University and Springer Nature Switzerland AG 2025

## Abstract

Drought events significantly influence the regional dynamics of crop growth conditions under climate change. In Bangladesh, the Ganges-Jamuna-Brahmaputra Floodplains are increasingly diminished by the rising frequency and severity of drought events, posing significant challenges to agricultural systems. This study investigates long-term drought dynamics using multi-source satellite data and drought indices to evaluate the spatial and temporal impacts of drought alongside climate-driven changes in water use efficiency (WUE) across the agricultural ecosystem. The Vegetation Health Index (VHI), Standardized Precipitation Index (SPI), and Advanced Drought Response Index (ADRI) were used to evaluate drought severity from 2002 to 2022. VHI quantifies agricultural drought, SPI measures meteorological drought using remote sensing precipitation data, and ADRI provides an advanced drought response perspective. The SPI shows mild droughts nearly every year, with extreme drought in 2006 and moderate-to-severe droughts in 2006, 2013, 2014, and 2018, when experienced below-average annual precipitation of 2337 mm. Satellite-derived SPI exhibited a strong and highly significant correlation with weather station observations ( $R^2 = 0.94$ ,  $p < 0.0001$ ). Additionally, MODIS-derived datasets were analyzed to explore the relationship between drought dynamics and WUE. Annual VHI trends indicated mild-to-moderate drought, with severe droughts in 2006, 2011, 2013, 2014, and 2016. Severe pre-monsoon droughts occurred in 2006, 2013, 2014, and 2018, while post-monsoon drought responses varied, benefiting *Boro* rice production in 2009, 2014, and 2018. The monsoon season remained largely drought-free due to sufficient rainfall. Strong correlations between VHI and ADRI ( $R^2 = 0.98$ ,  $p < 0.001$ ) and between SPI from remote sensing and weather station data ( $r = 0.94$ ,  $p < 0.0001$ ) validated the satellite-based approach. WUE averaged  $13.47 \text{ g C m}^{-2} \text{ mm}^{-1}$ , peaking at  $19.87 \text{ g C m}^{-2} \text{ mm}^{-1}$  in 2004 and reaching a low of  $7.11 \text{ g C m}^{-2} \text{ mm}^{-1}$  in 2002. These findings will contribute to mitigating drought impacts by enhancing agricultural strategies and refining climate change-focused agroecological zoning in Bangladesh and similar climatic regions across continental scales.

## Graphical Abstract

The graphical abstract provides an overview of the study on long-term drought impacts on agriculture in Bangladesh using multi-source remote sensing data. The background and conceptual framework illustrate how temperature and precipitation influence drought dynamics through ecosystem processes linked to soil moisture, evapotranspiration, photosynthesis, and vegetation health. Data from the Moderate Resolution Imaging Spectroradiometer (MODIS), Soil Moisture Active Passive (SMAP), Tropical Rainfall Measuring Mission (TRMM), and Global Precipitation Measurement (GPM) satellites, along with weather station data, were used to derive key environmental variables such as land surface temperature (LST),

Nur Hussain  
[nur.hussain@utoronto.ca](mailto:nur.hussain@utoronto.ca); [nurhussain55@gmail.com](mailto:nurhussain55@gmail.com)

Md Saifuzzaman  
[md.saifuzzaman@mail.mcgill.ca](mailto:md.saifuzzaman@mail.mcgill.ca)

Mohd. Shamsul Alam  
[m.s.alam.ju@juniv.edu](mailto:m.s.alam.ju@juniv.edu)

Md Shamim Ahamed  
[mahamed@ucdavis.edu](mailto:mahamed@ucdavis.edu)

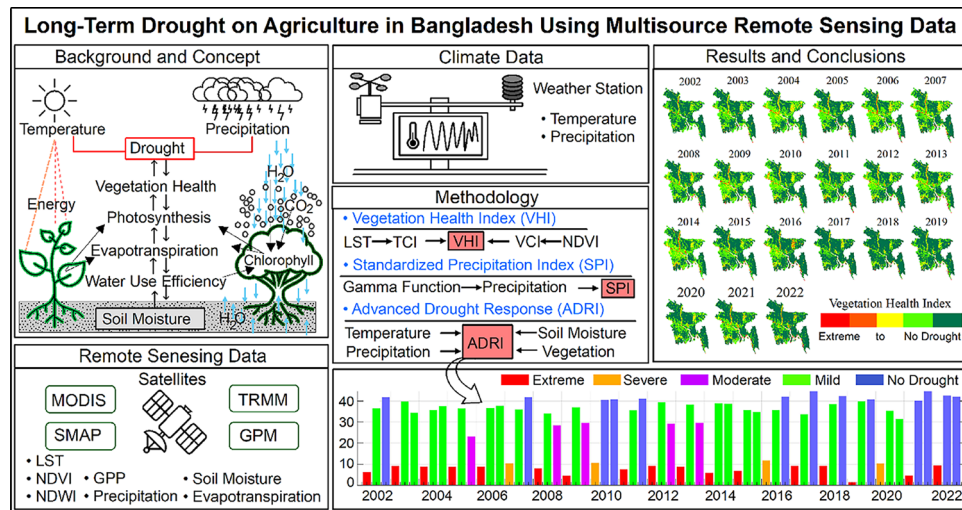
<sup>1</sup> Department of Biology, University of Toronto, 3359 Mississauga Road, Mississauga, ON L5L1C6, Canada

<sup>2</sup> Department of Biology, McGill University, Montreal, QC H3A 0G4, Canada

<sup>3</sup> Department of Geography & Environment, Jahangirnagar University, BangladeshSavar, Dhaka-1342, Bangladesh

<sup>4</sup> Department of Biological and Agricultural Engineering, University of California Davis, Davis, California, CA 95616, USA

normalized difference vegetation index (NDVI), normalized difference water index (NDWI), gross primary productivity (GPP), precipitation, soil moisture, and evapotranspiration (ET). The study employed three drought indices to explore drought dynamics: (i) the Vegetation Health Index (VHI), which incorporates the NDVI-based Vegetation Condition Index (VCI) and the LST-based Temperature Condition Index (TCI), (ii) the Standardized Precipitation Index (SPI) based on precipitation, and (iii) the Advanced Drought Response Index (ADRI), integrating temperature, soil moisture, precipitation, and vegetation parameters. Results from 2002 to 2022 reveal annual drought patterns, with spatial maps showing varying drought intensities and bar charts illustrating trends in VHI, SPI, and ADRI. In conclusion, the strong correlation  $R^2 = 0.94$ ;  $p < 0.001$ ) between satellite-based drought indices and weather station data underscores the critical role of temperature and precipitation in drought monitoring, highlighting the value of remote sensing for agricultural drought assessment.



## Highlights

- Remote sensing technology effectively explores drought dynamics.
- Drought indices evaluate the impact of climate extremes on agriculture.
- Severe drought events were detected in Bangladesh in 2006, 2011, 2013, 2014, and 2016.
- Remote sensing indices and weather station-measured drought are strongly correlated.
- Water use efficiency increases with drought severity, reflecting ecosystem adaptation.

**Keywords** Ecosystem · Climate extremes · Drought dynamics · Drought monitoring · Remote sensing · Spatiotemporal analysis · Water-use efficiency

## 1 Introduction

Drought is a complex environmental phenomenon characterized by longer periods of unusually low precipitation, resulting in water deficits that stress ecosystems and agriculture (Bhuiyan et al. 2006; Vicente-Serrano et al. 2020). Its impacts are extensive, affecting socioeconomic, agricultural, and environmental conditions and are often intensified by climate change, which is projected to increase the frequency and intensity of drought events globally (Viau et al. 2000; Bhuiyan et al. 2006; Jiao et al. 2016; Madakumbura et al. 2019; Saharwardi et al. 2022; Mannocchi 2023; Nugraha et al. 2023; Yildiz et al. 2024). Countries in tropical region, with both climatic and natural vulnerabilities, are particularly susceptible to these effects (Brammer

1987; Dewan 2015; Miyan 2015; Wilhite, 2015; Padrón et al. 2020). Drought occurs when soil moisture supply falls short of levels needed to sustain crop growth during the regular growing season and can be classified into several types: agricultural, meteorological, hydrological, and socio-economic (Nagarajan 2010; Wilhite et al. 2014; Karim and Rahman 2015; Wang et al. 2016; Kumar and Chu 2024). Agricultural drought specifically impacts vegetation health and productivity due to adverse climatic and hydrological factors, influencing ecosystems and agricultural systems and covering vegetation directly (Zhang and Jia 2013; Kohl and Knox 2016; Hazaymeh and Hassan 2017; Guria et al. 2025). As a key component of the country's environmental system and rural livelihoods, the agricultural ecosystem is particularly vulnerable to drought, which disrupts crop

cycles, reduces yields, and intensifies pressure on water and limited land resources (Sultana et al. 2023; Mamun et al. 2024).

Seasonal drought patterns demonstrate substantial variation across the globe, primarily due to diverse inter-regional climatic dynamics (Ahmed et al., 2020). Regional climate systems play a crucial role in determining the onset, intensity, and duration of droughts, influencing their manifestation at both macro and micro scales. Fluctuations in temperature, altered precipitation patterns, and changes in large-scale air movement systems affect local drought conditions, often intensifying or reducing their impacts depending on topographic and ecological variability (Chakraborty & Islam, 2018). In South Asia, for example, evolving monsoon behavior and regional climate warming have both contributed to heightened drought intensity and recurrence (Rahman et al., 2022). Developing effective drought monitoring systems, incorporating advanced technologies (e.g., remote sensing, derived indices) and designing adaptive strategies that respond to local conditions require a clear understanding of these complex interactions.

Drought indices provide quantifiable measures of drought conditions, simplifying this complex phenomenon into metrics that can be monitored over time (Al-Qinna et al. 2011; Shah et al. 2015). For example, the Standardized Precipitation Index (SPI) captures meteorological drought through precipitation density, while the Advanced Drought Response Index (ADRI), a multivariate index, integrates precipitation, soil moisture, vegetation condition, and temperature data for a more comprehensive drought assessment (Kogan 1995; WMO 2012; Bloomfield and Marchant 2013; Singh et al. 2022). The Vegetation Health Index (VHI), widely applied for monitoring agricultural drought, combines the Normalized Difference Vegetation Index (NDVI), Vegetation Condition Index (VCI), and Temperature Condition Index (TCI) (Kogan 1995; Gao 1996; Huang et al. 2020). Indices like the SPI, VHI, and ADRI offer essential insights for drought monitoring and resilience-building strategies, especially in drought-prone regions such as Bangladesh.

Over the last four decades, the NDVI has become a primary tool for detecting and monitoring vegetation, providing a measure of vegetation density and health (Carlson and Arthur 2000; Satyanarayana et al. 2011; Hussain and Islam 2020; Newton et al. 2024). The VCI, derived from the NDVI, assesses the impact of weather on vegetation, while the TCI, relying on land surface temperature (LST) data, reflects climatic conditions (Gitelson et al. 1998; Singh et al. 2003; Amri et al. 2011; Amalo and Hidayat 2017). VHI integrates the VCI and TCI, offering a robust metric for agricultural drought monitoring derived solely from remote sensing data independent of ground-based observations (Touma et al. 2015). The SPI, another widely used drought

index, quantifies meteorological drought by utilizing rainfall data over varying timescales (Guttman 1999; Domenikiotis et al. 2004; Zhao et al. 2018; Kumar et al. 2024). This study calculated SPI values using rainfall data from the Tropical Rainfall Measuring Mission (TRMM) satellite (Morris et al. 2007; Chen et al. 2020) and the weather station observed rainfall data, allowing comparisons with the VHI. While the SPI mainly reflects precipitation trends, the VHI is influenced by biomass characteristics, providing a broader view of agricultural drought impacts (Zambrano et al. 2016; Mondol et al. 2017; Winkler et al. 2017; Satoh et al. 2021; Harishnaika et al. 2022). However, the single-index drought assessments like SPI often overlook key factors such as vegetation stress, soil moisture, and climate-induced changes in water use efficiency (WUE). Remote sensing-based drought indices enable a more integrated view by capturing both meteorological and biophysical responses. This study employs a multi-index approach—comparing SPI, VHI, and ADRI—to provide a comprehensive assessment of drought impacts and their consequences on WUE and ecosystems.

Tropical countries, such as Bangladesh, face increasing vulnerability to climate-induced drought, with rising temperatures and shifting rainfall patterns heightening the risks (Shahid & Hazarika, 2010; Alamgir et al., 2015). Country's annual average maximum temperature rose by 0.16°C from 1994 to 2013, contributing to more frequent and severe droughts (Shahid & Behrawan, 2008; Rahaman et al., 2016). Historical records indicate major drought events at least once per decade, affecting over 39% of the country and half its population (Mishra & Singh, 2010; Shahid & Hazarika, 2010; Alamgir et al., 2015). Severe droughts, such as the 1978–1979 event, resulted in substantial crop losses, with approximately 2 million metric tons of rice damaged, underscoring the threat to food security (Brammer, 2014; Rahman et al., 2023).

Long-term climate trends further highlight the intensifying drought risk (Shamsuddin et al., 2020). Since 1950, surface temperatures have risen by 0.74°C, with recent observations showing a 1.16°C increase in maximum temperature between 1988 and 2017 (Mishra & Singh, 2010; Alamgir et al., 2015; Alam et al., 2023). Meanwhile, monsoon rainfall has declined in key agricultural regions, exacerbating water stress and reducing soil moisture availability (Brammer, 2014; Kamruzzaman et al., 2022). These climatic shifts have accelerated evapotranspiration, heightening agricultural droughts and threatening rice production, particularly Boro rice, which constitutes 55% of the country's total yield (MOF, 2010; Alam et al., 2023). Future projections indicate a 20% decline in Boro rice production by 2050 and up to 50% by 2070, primarily due to escalating heat stress, recurrent droughts, and intensified irrigation demands (Alam et al., 2023; Rahman et al., 2023; Islam yet

al., 2024). To mitigate these risks, some adaptation strategies such as improved irrigation, drought-resistant crop varieties, and sustainable water management are crucial for safeguarding food security (Shahid & Hazarika, 2010; Alamgir et al., 2015; Talukder et al., 2015).

Bangladesh's low-lying floodplain, is situated on the Himalayan River system deltas and experiences a tropical humid climate with distinct seasonal variations (Jahangir Alam et al. 2014; Mohsenipour et al. 2018). The country's climate is divided into three main seasons: pre-monsoon (January–April), monsoon (May–August), and post-monsoon (September–December), with over 75% of annual rainfall occurring during the monsoon. The agricultural cycle is divided into the Kharif season (May–October), which relies on monsoon rainfall, and the Rabi season (November–April), which depends primarily on groundwater irrigation (Alamgir et al. 2015). Agriculture is a cornerstone of Bangladesh's economy, accounting for around one-third of the GDP and involving approximately 60% of the labor force. Drought affects 0.574–1.748 million hectares of rice crops annually, posing significant socioeconomic challenges (Jahangir Alam et al. 2014). Projections by the Intergovernmental Panel on Climate Change (IPCC) suggest a potential global temperature rise of up to 7 °C by 2100, which would significantly heighten drought risks, especially in vulnerable countries like Bangladesh (Solomon et al. 2007; ADB 2012; Ahamed et al. 2017; Rayhan and Afroz 2024). Effective drought monitoring is thus essential for sustainable development and resilience (Sarkar et al. 2024; Hasan et al. 2024).

This study investigates a novel approach to drought monitoring in Bangladesh by integrating several remote sensing-based drought indices, including SPI, VHI, and ADRI (Kogan 1995; WMO 2012; Bloomfield and Marchant 2013; Singh et al. 2022). These indices offer a more comprehensive, multidimensional understanding of drought conditions, enabling a more nuanced analysis of agricultural and meteorological droughts. By examining a 21-year span (2002–2022), the study offers important insights into the spatiotemporal patterns of droughts in Bangladesh, a region particularly susceptible to climate change (Brammer 1987; Dewan 2015; Miyan 2015; Wilhite, 2015; Padrón et al., 2020). Our research fills a critical gap in the literature by incorporating advanced remote sensing techniques and newly developed drought response indices, offering a robust framework for informing more effective adaptation strategies to mitigate future drought impacts.

The primary objective of this study is to assess drought dynamics in Bangladesh using multi-source remote sensing data. While previous studies have primarily focused on meteorological drought (Al Mamun et al. 2024; Tahasin et al. 2024), this research combines SPI-based meteorological

drought with VHI-based agricultural drought and the multivariate ADRI to offer a more comprehensive view of drought conditions. Specifically, the SPI quantifies precipitation impacts, the VHI assesses drought effects on vegetation through changes in temperature and biomass, and the ADRI captures the combined effects of precipitation, soil moisture, vegetation health, and temperature. The research aims to (i) quantify annual and seasonal agricultural and meteorological drought conditions over the study period, (ii) compare agricultural and meteorological drought indices with ADRI and WUE, and (iii) analyze the influence of key climatic factors on drought events. Using Geographic Information System (GIS) tools, time-series drought maps based on NDVI, VCI, TCI, VHI, and SPI will be created to visualize the progression of drought patterns across Bangladesh.

## 2 Materials and methods

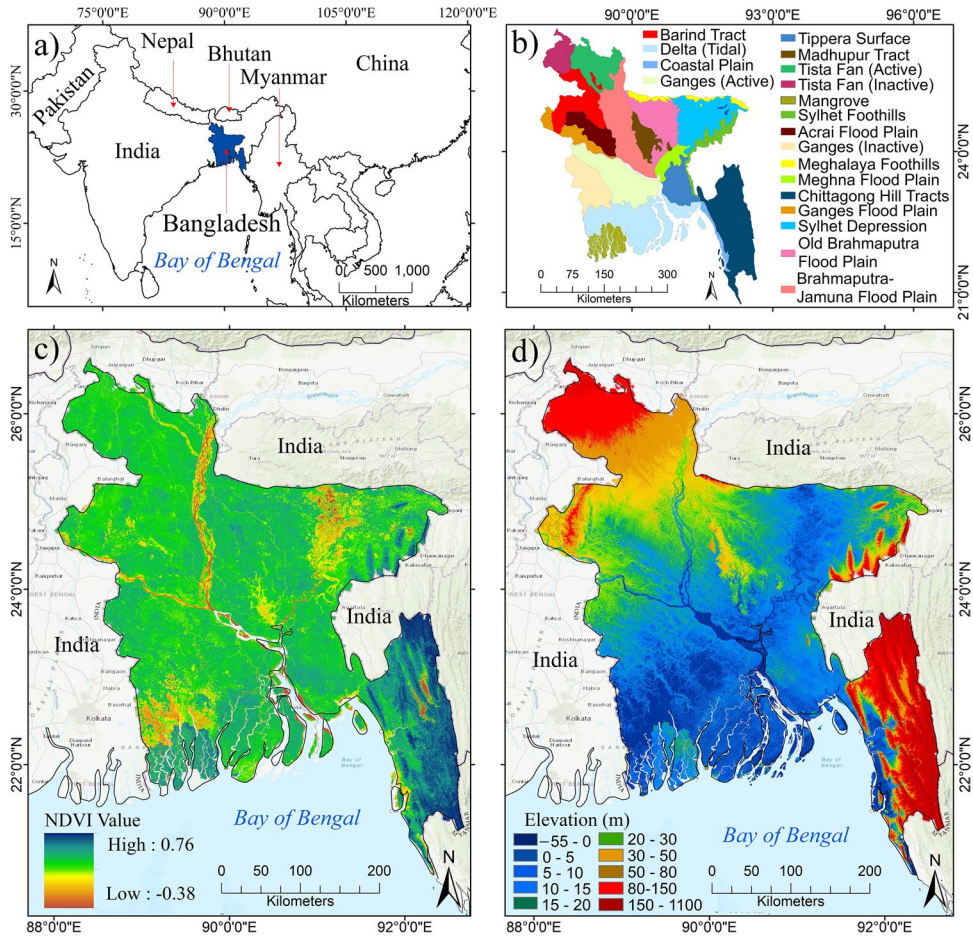
### 2.1 Study Area

The study area, Bangladesh, spans from 20°34' to 26°38' N latitude and 88°01' to 92°41' E longitude in South Asia (Fig. 1). Geopolitically, it is bordered by the Bay of Bengal to the south, surrounded on three sides by Indian states, and shares a small southeastern border with Myanmar (Fig. 1). Bangladesh covers approximately 144,000 km<sup>2</sup> of its total 147,570 km<sup>2</sup>, predominantly comprising low-lying floodplains shaped by sediment deposits from the Himalayas. This geographic setting makes the country particularly susceptible to severe climate change impacts. Bangladesh undergoes a tropical humid climate with moderately high temperatures and humidity, characterized by marked variability in air pressure, wind direction, rainfall, and temperature. The country has three distinct seasons: a hot pre-monsoon summer from January to April, a rainy monsoon season from May to August, and a dry winter from September to December (Hussain et al. 2017, 2021). Seasonal climatic shifts and the country's physiographic features play a crucial role in shaping agricultural productivity and vegetation growth, which rely on soil moisture and elevation variability (Wan, 1999). With an average elevation of 28 m, the terrain rises to its highest point at 1050 m in the southeastern hills, while much of the landscape lies within the Ganga-Brahmaputra-Meghna floodplain, often below 10 m above sea level (Fig. 1.d).

### 2.2 Satellite Data

This study utilizes multidimensional satellite data from various sources, including the Moderate Resolution Imaging Spectroradiometer (MODIS), the Tropical Rainfall

**Fig. 1** Detailed study area map: (a) The location map of Bangladesh, (b) Generalized Agroecological Map of Bangladesh (United States Geological Survey 2021); (c) Vegetation indices map of Bangladesh, showing the average vegetation condition of the previous 21 years spanning from 2002 to 2022, and (d) the elevation profile map of Bangladesh. The elevation data were collected from the United States Geological Survey (USGS) shuttle radar topography mission (SRTM) digital elevation model data inventory (approximately 30 m resolution), available at <https://earthexplorer.usgs.gov/>; accessed on 20 July 2024



Measuring Mission (TRMM), the Global Precipitation Measurement (GPM) (Skofronick-Jackson et al. 2018), and the Soil Moisture Active Passive (SMAP). Vegetation data, specifically the Normalized Difference Vegetation Index (NDVI), was obtained from the MODIS Vegetation Indices (MOD13Q1) Version 6, which provides 250 m resolution data at 16-day intervals. Temperature data were sourced from the MODIS Land Surface Temperature (LST) (MOD11A1) Version 6 daily dataset with a spatial resolution of 1 km (Wan, 1999). Additionally, MODIS Gross Primary Productivity (GPP) and evapotranspiration (ET) data were used to calculate water-use efficiency (WUE). GPP data were collected at 8-day intervals with a 500 m resolution, while ET data were obtained at the same interval with a spatial resolution. The MODIS-based datasets were sourced from the Goddard Space Flight Center (Maryland, USA) data site (<https://modis.gsfc.nasa.gov/data/>; accessed on 20 July 2024), precipitation data (TRMM and GPM) were obtained from the NASA global precipitation data site (<https://gpm.nasa.gov/data/directory>; accessed on 10 August 2024), and SMAP data were downloaded from the NASA's Jet Propulsion Laboratory (California Institute of Technology, California, USA) data site (<https://smap.jpl.nasa.gov/data/>; accessed on

10 August 2024). Additionally, we obtained weather station data from the Bangladesh Meteorology Department (BMD), for the period 2002–2022, to analyze the weather station-based SPI across Bangladesh.

Despite the limitations of weather stations and the lack of high-quality data, the comparison between station-based and satellite observations shows adequate agreement in temperature and precipitation (Table 1). The mean ground-measured temperature and satellite-derived land surface temperature (LST) were 30.7 °C and 27.27 °C, respectively, reflecting expected differences between air and surface temperature measurements. For precipitation, the mean values from weather stations and satellite observations were 204.1 mm and 194.8 mm, respectively. The standard deviations for temperature and precipitation were 2.73 °C and 2.3 °C, and 206.5 mm and 184.7 mm, respectively, indicating that both datasets captured temporal variability well. These results support the use of satellite data for drought monitoring while acknowledging limitations in spatial resolution and ground station coverage.

**Table 1** Comparison of basic statistical parameters (mean, maximum, minimum, and standard deviation) between weather station measurements and satellite observations for temperature (°C) and precipitation (mm)

Variable	Source	Mean	Maximum	Minimum	Standard Deviation	Correlation (Significant)
Temperature (°C)	Weather Station	30.7	35.5	24.3	2.73	0.98
	Satellite	27.27	32.5	21.45	2.3	( $P < 0.0001$ )
Precipitation (mm)	Weather Station	204.1	839.5	0.44	206.5	0.96
	Satellite	194.8	768.9	0.72	184.7	( $P < 0.0001$ )

## 2.3 Data Processing Methods

We analyzed temperature, evapotranspiration (ET), precipitation, and soil moisture data to evaluate the climatic conditions. Temperature data were obtained from the MODIS-LST products, complemented by observed temperature data from 25 weather stations of the Bangladesh Meteorological Department (BMD). ET data were derived from the MODIS (MOD16A2) dataset, which provides ET values at a 500 m spatial resolution and an 8-day interval. All satellite datasets were selected for their consistent temporal coverage and proven suitability for drought and vegetation monitoring from 2002 to 2022, with data acquired at 8-day or 16-day intervals depending on the product and resampled to a common spatial resolution of 500 m to ensure inter-product consistency with monthly and seasonal aggregation. To enhance data quality, we excluded MODIS scenes with more than 10% cloud cover using the quality assurance (QA) flags included in each product. Multi-source satellite data corrected for atmospheric effects to ensure accurate vegetation index calculations (e.g., NDVI, NDWI) in ArcGIS Pro (Version 3.5; Esri, Inc., California). Geometric correction was then conducted in ArcGIS Pro to align all datasets spatially, temporally, reprojecting the MODIS imagery from its native Sinusoidal projection to the WGS 84 coordinate reference system using bilinear interpolation for consistency with other data sources such as SMAP soil moisture and TRMM, GPM precipitation data.

Soil moisture data, essential for understanding drought conditions, were captured from the SMAP mission, facilitated by NASA's Hydrological Science Laboratory in collaboration with the USDA Foreign Agricultural Service, covering the period from 2010 to 2020. The SMAP soil moisture data provides direct measurements of surface water availability, while the MODIS-derived Normalized Difference Water Index (NDWI) serves as a spectral indicator reflecting surface water and near-surface soil moisture conditions (Giese et al. 2025). Our analysis revealed a strong correlation between NDWI and SMAP soil moisture ( $R^2 = 0.82$ ,  $p < 0.001$ ), highlighting their shared sensitivity to drought-induced variations in water availability. This is consistent with previous findings that demonstrated NDWI's reliability in capturing soil moisture patterns in various agroecological contexts (Gu et al. 2008; Hosseini

and Saradjian 2011). NDWI has been widely used to estimate soil moisture due to its responsiveness to vegetation water content and surface wetness, making it particularly useful when direct measurements (e.g., from SMAP) are unavailable (Leng et al. 2017; Giese et al. 2025). Therefore, in this study, NDWI was employed to reconstruct missing soil moisture values prior to the SMAP record, enhancing the continuity of drought-related analyses across the 2002–2022 period.

Precipitation data were captured from the Tropical Rainfall Measuring Mission (TRMM), with missing values filled using the Global Precipitation Measurement (GPM) dataset, along with observed rainfall data from 25 weather stations across Bangladesh, provided by the BMD. This comprehensive dataset confirmed continuous and reliable climatic data, supporting a robust analysis of long-term climatic trends. The research design is illustrated in Fig. 2. To contextualize our methodology and highlight its comparative value, we synthesized previous major drought studies in Bangladesh alongside the present study in Table 5, summarizing key methods, spatial-temporal coverage, and major findings on seasonal variability and climate change impacts.

## 2.4 Estimation of Agricultural Drought

Agricultural drought was assessed using the VHI, derived from smoothed averages of the Vegetation Condition Index (VCI) and Temperature Condition Index (TCI) for the study area, analyzed across pre-monsoon, monsoon, and post-monsoon periods from 2002 to 2022. The VCI was calculated at a spatial resolution of 500 m with biweekly smoothing, while the TCI was generated at 500 m spatial resolution with biweekly smoothing (Kogan 1995, 2002). VHI maps were created by integrating both VCI and TCI data to capture agricultural drought intensity. The VCI classified agricultural drought into five categories provided in Table 2. Based on these categories, agricultural drought maps were produced to illustrate the spatial and temporal distribution of drought across the study area. The values of VCI, brightness temperature (BT), TCI, and VHI are presented as follows (Kogan 1995; Gitelson et al. 1998; Amalo and Hidayat 2017):

**Fig. 2** The experimental design of the research. Here, SMAP is Soil Moisture Active Passive, TRMM is Tropical Rainfall Measuring Mission, GPM is Global Precipitation Measurement, MODIS is Moderate Resolution Imaging Spectroradiometer, NDVI is the Normalized Difference Vegetation Index, NDWI is the Normalized Difference Water Index, GPP is Gross Primary Productivity, LST is land surface temperature, ET is evapotranspiration, WUE is water-use efficiency, VCI is the Vegetation Condition Index, TCI is the Temperature Condition Index, SCI is the Soil Condition Index, PCI is the Precipitation Condition Index, VHI is the Vegetation Health Index, SPI is the Standardized Precipitation Index, and ADRI is the Advanced Drought Response Index

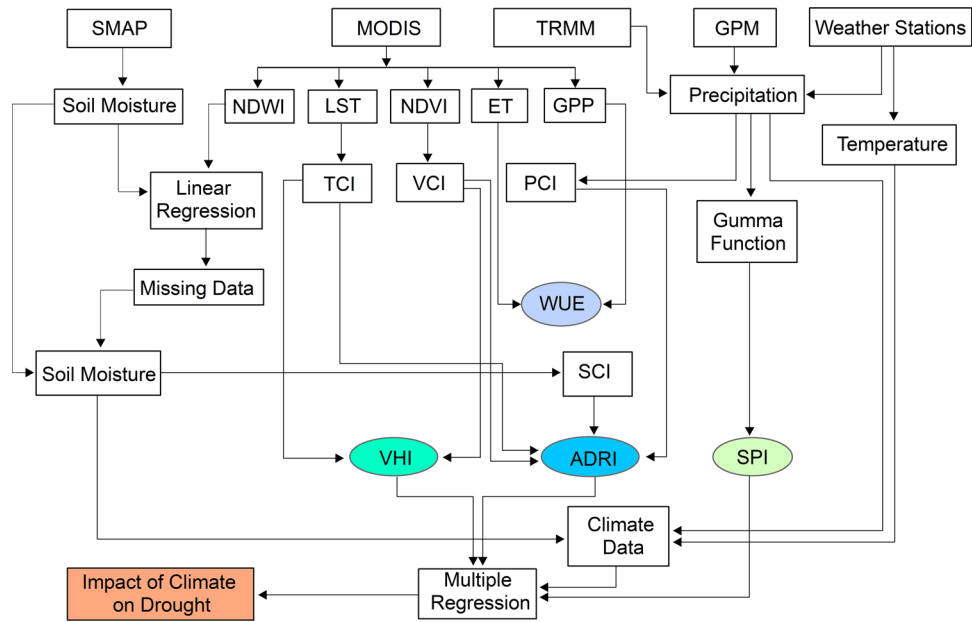


**Table 2** Categorization of different drought intensity levels using three indicators: meteorological drought (Standardized precipitation index – SPI), agricultural drought (Vegetation health index – VHI), and the composite advance drought response index (ADRI)

Types of Drought Events	Meteorological Drought (SPI)	Agricultural Drought (VHI)	Advanced Drought Response Index (ADRI)
Extreme Drought	Below -2.0	Below 10,	Below 10,
Severe Drought	-2.1 to -1.50	10.1–20	10.01–20
Moderate Drought	<-1.51 to -1.0	20.1–30	20.1–30
Mild Drought	<-1.0 to 0	30.1–40	30.1–40
No Drought	0 Above	40 Above	40 Above

$$VCI = 100 \times \frac{NDVI - NDVI_{min}}{NDVI_{max} - NDVI_{min}} \quad (1)$$

Where, VCI represents the Vegetation Condition Index, and NDVI is the seasonal average of smoothed biweekly NDVI values.  $NDVI_{max}$  and  $NDVI_{min}$  represent the multi-year absolute maximum and minimum NDVI, respectively.

$$BT = (LST \times SF) - 273.15 \quad (2)$$

Where, BT is the seasonal average of the weekly smoothed brightness temperature ( $^{\circ}\text{C}$ ),  $BT_{max}$  is the multi-year absolute maximum BT, and  $BT_{min}$  is the multi-year absolute minimum BT. LST denotes land surface temperature in Kelvin, the scaling factor (SF) is set to 0.02 for MODIS MOD09A1 V6.

$$TCI = 100 \times \frac{BT_{max} - BT}{BT_{max} - BT_{min}} \quad (3)$$

Where, TCI is the Temperature Condition Index, reflects relative changes in thermal conditions based on brightness temperature, with values derived from MODIS MOD09A1 V6 land surface reflectance, smoothed over 8-day intervals, to generate LST data for the period 2002–2022.

$$VHI = (0.5 \bullet VCI) + (0.5 \bullet TCI) \quad (4)$$

Where, VHI is Vegetation Health Index, VCI represents the Vegetation Condition Index and TCI is the Temperature Condition Index.

## 2.5 Estimation of Meteorological Drought

The SPI (McKee et al. 1993; WMO 2012) is widely recognized for assessing long-term meteorological droughts, particularly those that emerge over seasonal timescales. In this study, spatiotemporal analyses were performed using SPI to evaluate its effectiveness as a meteorological drought index for the region. A detailed summary of SPI values is presented in Table 2, where negative values indicate dry conditions and positive values reflect wet conditions (Saharwardi et al. 2021).

SPI is a robust metric for quantifying drought based on precipitation anomalies. For this analysis, SPI was calculated using precipitation data from a total of 25 weather stations operated by the Bangladesh Meteorological Department (BMD), along with satellite-derived precipitation datasets from TRMM and GPM. SPI values were computed by normalizing the deviation of seasonal precipitation from the long-term mean, applying a gamma distribution function in accordance with WMO (2012) and Bloomfield and Marchant (2013).

$$SPI = \frac{X_{ij} - X_{im}}{\delta} \quad (5)$$

where  $X_{ij}$  is the seasonal rainfall,  $X_{im}$  is the long-term seasonal mean, and  $\delta$  is the standard deviation of  $X_{im}$ .

## 2.6 Estimation of Advance Drought Response Index

In this study, we utilized the ADRI to analyze climatic responses to drought conditions, integrating remote sensing-based soil moisture, precipitation, vegetation health, and temperature condition data. The ADRI is composed of the VCI, TCI, Precipitation Condition Index (PCI), and Soil Condition Index (SCI) (Kogan 1995; USDA-NRCS 2003; Duet al. 2013; Zeng et al. 2023). ADRI values near 0 indicate extreme drought conditions characterized by stressed vegetation, low precipitation, and elevated temperatures, while values approaching 100 represent normal conditions with healthy vegetation, sufficient precipitation, and favorable temperatures (Kogan 1995). The VCI is derived from remotely sensed vegetation data, while the TCI, PCI, and SCI are calculated based on temperature, precipitation, and soil moisture observations, respectively, as described by the following equations (Kogan 1995; WMO 2012; Bloomfield and Marchant 2013; Singh et al. 2022).

$$ADRI = \left[ L * VCI * \left\{ c + \frac{1}{L * (VCI + TCI + PCI + SCI + C)} * (TCI + PCI + SCI) \right\} \right] \quad (6)$$

$$PCI = 100 * \frac{(P_{max} - P_{min})}{(P_{max} - P_{min})} \quad (7)$$

$$SCI = 100 * \frac{(SM - SM_{min})}{(SM_{max} - SM_{min})} \quad (8)$$

Where, ADRI represents the advanced drought response index,  $L$  is the normalization factor (set to 0.25) to ensure the output value falls within the expected range, and  $c$  is a constant (set to 0.01) (Singh et al. 2022). The normalization factor  $L$ , set at 0.25, is used to scale the ADRI values so they remain within a standardized and interpretable range, facilitating consistent comparison across different datasets and time periods (Singh et al. 2022). This value helps balance sensitivity and stability in the index, avoiding exaggerated fluctuations caused by extreme environmental changes. The constant  $c$ , set to 0.01, serves as a small offset to prevent division by zero or undefined values during calculations, ensuring numerical stability especially when observed variables approach their minimum or maximum limits. Together,  $L$  and  $c$  enhance the robustness and reliability of the ADRI by maintaining consistent output and avoiding

computational errors. VCI denotes the Vegetation Condition Index, TCI represents the Temperature Condition Index, and PCI stands for the Precipitation Condition Index.  $P$  is precipitation, with  $P_{min}$  and  $P_{max}$  as the minimum and maximum precipitation values observed over the study period. SCI is the Soil Condition Index, where  $SM$  represents soil moisture, with  $SM_{min}$  and  $SM_{max}$  indicating the minimum and maximum soil moisture values during the study period. A detailed summary of the different drought index categories and their representations is presented in Table 2.

## 2.7 Water-Use Efficiency (WUE)

Water-use efficiency (WUE) is a critical metric for assessing ecosystem responses to drought stress across different severities and vegetation types (Wilhite 2016; Hussain et al. 2022). WUE measures the amount of carbon assimilated into biomass per unit of water used by vegetation (Hatfield and Dold 2019). At the ecosystem level, WUE is a valuable ecological indicator, capturing the interaction between carbon and water balances. It is defined as the ratio of carbon sequestration to water lost through processes like photosynthesis and transpiration. In this study, we utilized Gross Primary Productivity (GPP) and evapotranspiration (ET) data

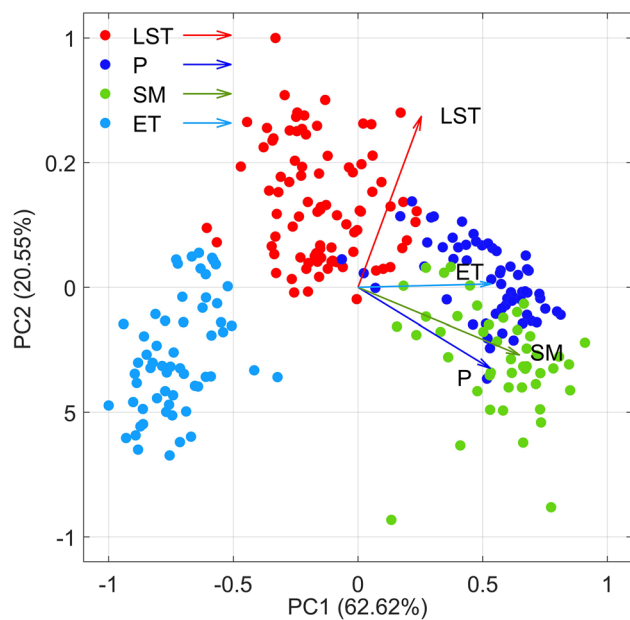


**Fig. 3** Principal Component Analysis (PCA) of climate data and water balance. LST represents Land Surface Temperature,  $P$  denotes the monthly mean precipitation, while the other variables include Soil Moisture (SM) and Evapotranspiration (ET)

from the MODIS dataset (Das et al. 2023; Du et al. 2024). A comparative analysis of WUE was conducted across various drought indices, and temporal trends in WUE were analyzed using Eq. 9. Statistical analyses were performed to calculate and compare correlations between drought occurrences and WUE across different drought types.

$$WUE = \frac{GPP}{ET} \quad (9)$$

where, WUE is water-use efficiency ( $\text{g C m}^{-2} \text{ mm}^{-1}$ ), GPP is the Gross Primary Productivity ( $\text{g C m}^{-2}$ ) and ET is evapotranspiration retrieved from MODIS satellite data.

## 2.8 Statistical Analysis

A two-dimensional principal component analysis (PCA) was performed to assess the quality and variability of climatic data, using monthly mean values from 2002 to 2022 to identify dominant patterns and potential inconsistencies (Jollife, and Cadima, 2016); Hussain et al. 2024). The PCA results were visualized in a biplot, where the first principal component (PC1) explained 66.62% of the variance, while the second principal component (PC2) accounted for 20.55%, together capturing 83.17% of the total variation (Fig. 3).

To further investigate the relationships between drought and key climatic factors, a multiple linear regression model was used. In this model, drought indices served as the response variable, while climatic variables such as temperature (LST), soil moisture, and precipitation acted as predictors. The multiple linear regression model is represented by Eq. (10) (Shewhart et al. 2003; Kutner et al. 2004). Additionally, the correlation coefficient for individual variables was calculated using Eq. (11).

$$Y_i = \beta_0 + \beta_1 X_{i1} + \beta_2 X_{i2} + \dots + \beta_p X_{ip} + \epsilon_i, \quad i = 1, \dots, n \quad (10)$$

$$R^2 = \frac{\sum_{i=1}^n (y_i - \bar{y})^2}{\sum_{i=1}^n (y_i - \bar{y})^2} \quad (11)$$

Where  $n$  is the number of observations,  $y_i$  is the  $i$ th response, is the response variable, and  $1, 2, \dots, X_{i1}, X_{i2}, \dots, X_{ip}$  are the predictor variables.  $0$  is the intercept, and  $1, 2, \dots, \beta_1, \beta_2, \dots, \beta_p$  are the coefficients that indicate the influence of each predictor on  $y$ .  $\epsilon_i$  represents the error term, capturing the difference between observed and predicted values. The model estimates these coefficients to minimize the error across all observations.

## 3 Results

### 3.1 Seasonal Climate Patterns

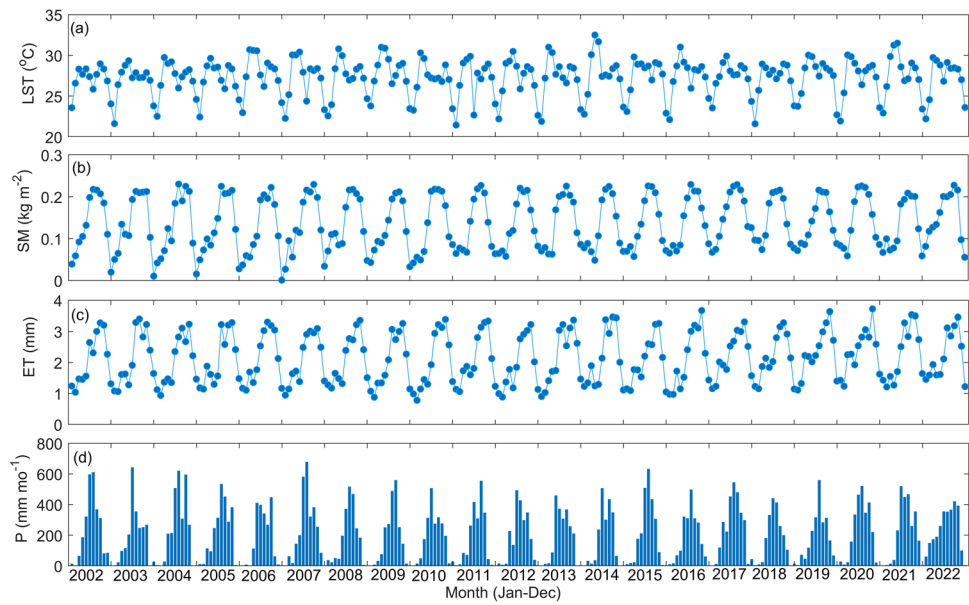
Meteorological variables, including temperature LST, were analyzed using satellite data from MODIS, TRMM, GPM, and SMAP over the period 2002–2022 (Figs. 4 and 5). The monthly average LST during this period was  $27.27 \pm 2.3$  °C. The highest monthly LST was observed in April 2014 at 32.5 °C, while the lowest was recorded in January 2011 at 21.44 °C. Seasonal temperature fluctuations followed typical regional patterns, with peak LST in April and May, averaging  $29.85 \pm 1.05$  °C and  $29.49 \pm 1.13$  °C, respectively, and the lowest temperatures in December ( $23.75 \pm 0.59$  °C) and January ( $22.6 \pm 0.68$  °C) (Fig. 4a).

In 2022, the yearly average soil moisture for Bangladesh was  $0.1520 \text{ kg/m}^2$ , which is above the long-term average of  $0.1358 \text{ kg/m}^2$ , reflecting wetter conditions (Fig. 4.b). The soil moisture pattern shows significant seasonality, with the lowest levels recorded in January ( $0.0609 \text{ kg/m}^2$ ) and December ( $0.0584 \text{ kg/m}^2$ ), marking the dry season. Moisture levels increase in April ( $0.0976 \text{ kg/m}^2$ ) as the pre-monsoon rains start and peak in July ( $0.2155 \text{ kg/m}^2$ ), reflecting the monsoon's peak rainfall. The post-monsoon months show a decline in soil moisture, with September at  $0.2119 \text{ kg/m}^2$  and further drops in October ( $0.1814 \text{ kg/m}^2$ ) and November ( $0.1085 \text{ kg/m}^2$ ). This seasonal variation emphasizes the significant role of the monsoon in replenishing soil moisture and highlights the need for effective water management strategies during dry months (Islam et al. 2024). Dry years, such as 2006 and 2018, show declining soil moisture, indicating potential challenges for agriculture and ecosystem stability. Integrating satellite-based climate monitoring with localized weather data can improve drought and flood

forecasting, aiding sustainable land and water management in Bangladesh.

Evapotranspiration (ET) patterns, derived from MODIS data, revealed the monthly average ET rate of  $2.12 \pm 0.81 \text{ mm d}^{-1}$ , with a peak of  $2.35 \text{ mm d}^{-1}$  in 2020 and a low of  $1.93 \text{ mm d}^{-1}$  in 2012. ET showed distinct seasonal patterns, with October reaching the highest monthly ET at  $3.33 \text{ mm d}^{-1}$ , attributed to high post-monsoon radiative energy and sufficient soil moisture. In contrast, the lowest ET levels were in January ( $1.15 \text{ mm d}^{-1}$ ) and February ( $1.11 \text{ mm d}^{-1}$ ), coinciding with reduced daylight and radiative energy (Fig. 5c). Surface-level soil moisture across the

**Fig. 4** Monthly time series of mean (a) land surface temperature (LST) in °C, (b) soil moisture (SM) in  $\text{kg m}^{-2}$ , and (c) evapotranspiration (ET) in mm and (d) monthly total precipitation (mm) from 2002 to 2022



study area averaged  $0.135 \pm 0.06 \text{ kg m}^{-2}$  or 13.5% per land unit, with peak moisture levels of 15.7% in 2017 and a minimum of 12% in 2006. Seasonal variations were evident, with soil moisture reaching maximum levels from July to September (0.215, 0.214, and 0.212  $\text{kg m}^{-2}$ , respectively), while the lowest levels occurred in December (0.05  $\text{kg m}^{-2}$ ) and January (0.06  $\text{kg m}^{-2}$ ), aligning closely with precipitation trends (Fig. 4.b).

The study area's long-term average annual precipitation was 2337 mm, with notable dry years (2006, 2009, 2013, 2014, and 2018) characterized by precipitation anomalies below 10% of the average, and wet years (2002, 2004, 2007, 2017, and 2022) exhibiting anomalies above 10%

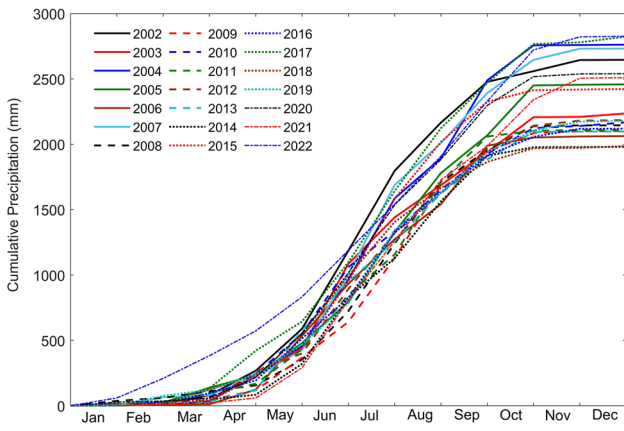


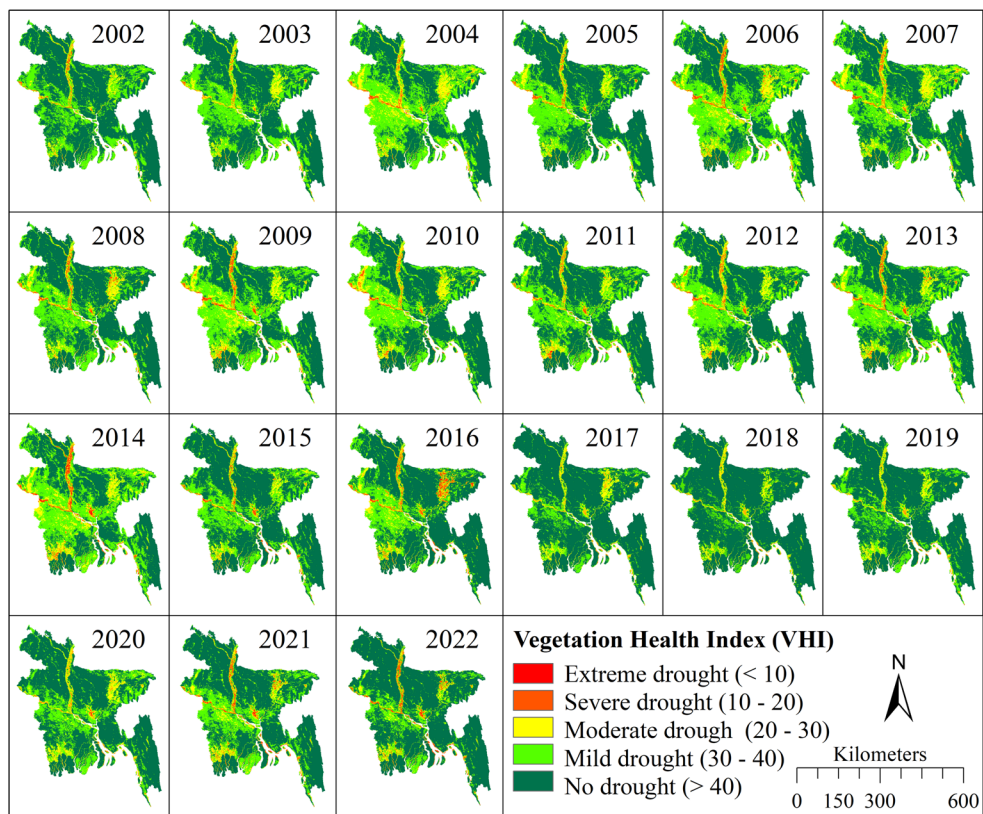
**Fig. 5** Monthly cumulative precipitation (P) from 2002 to 2022. The yearly precipitation was calculated from the Tropical Rainfall Measuring Mission (TRMM) and the Global Precipitation Measurement (GPM) dataset composited monthly. The highest precipitation was recorded in 2002 (2646 mm), 2004 (2761 mm), 2007 (2731 mm), 2017 (2823 mm), and 2022 (2825 mm); conversely, the lowest precipitation was recorded in 2006 (2062 mm), 2009 (2101 mm), 2013 (2098 mm), 2014 (1980 mm), and 2018 (1986 mm)

(Fig. 5). The highest annual precipitation occurred in 2017 (2823 mm) and 2022 (2825 mm), while the lowest was in 2014 (1980 mm) and 2018 (1886 mm). The monsoon season (May–August) was the predominant contributor, accounting for 67% of the annual rainfall, with the remaining 33% distributed annually. July had the highest average monthly rainfall at 464 mm, while December (7 mm) and January (10 mm) were the driest months.

### 3.2 Agricultural Drought and Regional Variability

The annual calculation of the VHI from 2002 to 2022 revealed consistent mild-to-moderate drought conditions in Bangladesh, with severe droughts recorded in 2006, 2011, 2013, 2014, and predominantly in 2016 (Fig. 6). In 2016 alone, extreme to severe drought conditions affected approximately 13,848 km<sup>2</sup>—about 13% of the country's total agricultural land—posing serious threats to crop production and rural livelihoods. Geomorphologically vulnerable regions such as the *Char* (riverbanks or islands) areas along riverbanks were significantly impacted due to their sandy, well-drained soil and limited irrigation infrastructure, exacerbating water retention issues. Similarly, the northeastern *Haor* (wetland) regions faced pronounced drought during dry seasons (December to January), further intensifying their vulnerability due to their dependence on irrigation for rice cultivation (Baishakhy et al. 2023). The northwest and southeast zones of Bangladesh emerged as hotspots for agricultural drought intensity. The northwestern Himalayan piedmont zone and southeastern Tertiary hill regions are particularly susceptible due to climatic factors and reduced river flow. Annual droughts in northern areas result from diminished river discharge in the Tista, Ganges,

**Fig. 6** Spatial distribution of annual agricultural drought from 2002 to 2022. The maps present the Vegetation Health Index (VHI) classified by five agricultural drought levels of  $<10$ ,  $10\text{--}20$ ,  $20\text{--}30$ ,  $30\text{--}40$ , and  $>40$ , considered extreme, severe, moderate, mild, and no drought intensity, respectively (Zeng et al. 2023)



and Brahmaputra rivers, often linked to upstream water dams. These regions, locally referred to as “Monga areas”, experience seasonal food insecurity and severe agricultural disruptions due to recurrent drought conditions.

The results highlight the persistent susceptibility of Bangladesh to agricultural drought, which is driven by climatic, geomorphic, and hydrological factors. *Haor* and *Char* areas are particularly exposed to seasonal drought and flooding, illustrating a dual vulnerability that complicates agricultural planning and water resource management for government authorities (Rahman 2018; Sarkar et al. 2024). The reliance on irrigation in the northeastern wetlands intensifies the impact of water scarcity during dry periods, while the northwest’s dependence on reduced river flows exacerbates drought severity in the Monga areas (Rahman, 2018); Das et al. 2023).

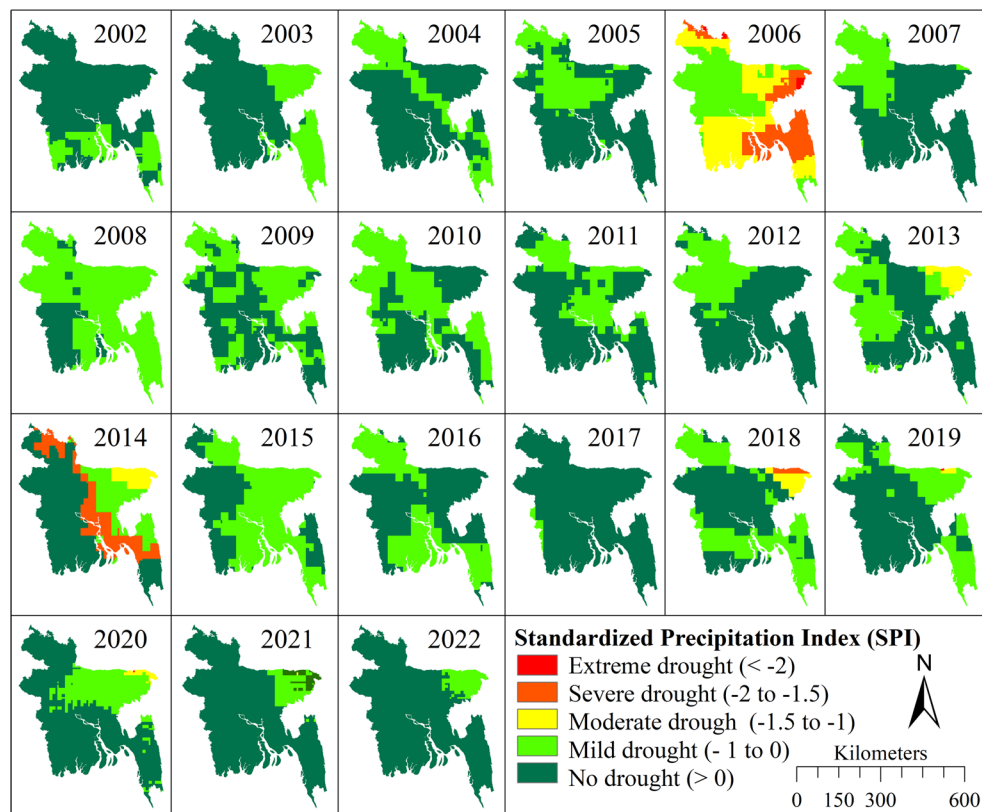
The interchange of upstream water management, geomorphic soil properties, and local climatic conditions creates a complex mixture of drought vulnerability across Bangladesh. Effective mitigation strategies should improve irrigation infrastructure, enhance water retention in sandy soils, and adopt sustainable water-sharing practices in trans-boundary river basins (Alamgir et al. 2015; Al Maman et al. 2024). Targeted interventions in the northwest and southeast regions are critical to alleviating the impacts of recurring droughts and ensuring food security in these highly affected zones.

Elevated LST during dry months further intensifies agricultural drought by accelerating evapotranspiration and reducing soil moisture reserves. These thermal dynamics are especially detrimental in already water-stressed regions. The Temperature Condition Index (TCI), derived from satellite-based brightness temperatures, provides a valuable metric for quantifying this stress by comparing current LST to historical extremes. Low TCI values reflect higher thermal stress and vegetation vulnerability, while higher TCI values suggest more favorable growing conditions. In this study, MODIS LST data (2002–2022) demonstrated a moderate but statistically significant relationship with drought intensity ( $R^2 = 0.45$ ,  $p < 0.0001$ ), confirming TCI’s utility as a thermal proxy for vegetation health. Integrating such indices with climate projections can enhance the predictive capacity of drought monitoring systems, supporting effective agricultural planning under future climate uncertainty.

### 3.3 Spatiotemporal Meteorological Drought

Rainfall data from TRMM and GPM satellites were analyzed using geospatial and geostatistical methods to investigate the spatiotemporal variability of meteorological drought across Bangladesh from 2002 to 2022 (Fig. 7). The SPI highlighted mild drought events occurring almost annually, with extreme meteorological drought localized in 2006. Moderate-to-severe droughts were observed in 2006, 2013,

**Fig. 7** Spatial distribution of meteorological drought in Bangladesh. The maps show the Standardized Precipitation Index (SPI) classified by five categories of meteorological drought level: (i)  $<-2.0$ , (ii)  $<-1.5$ , (iii)  $<-1.0$ , (iv)  $<0$ , and (v)  $>0$ , considered as extreme, severe, moderate, mild, and no drought intensity, respectively (Gupta et al. 2022)



2014, and 2018, coinciding with annual precipitation deficits compared to the average of 2337 mm. Precipitation levels dropped to 2062 mm (2006), 2098 mm (2013), 1980 mm (2014), and 1986 mm (2018), exacerbating drought severity during these years. Spatially, droughts were concentrated in the northwest to northeast regions, where higher elevations and *Char* areas with poorly water-retentive soils heightened vulnerability. Seasonal precipitation distribution further illustrates the dominance of the monsoon season, with July contributing significantly to annual rainfall, while dry periods in December and January underscored the challenge of water scarcity during non-monsoon months (Shamsuddin et al. 2020).

The findings emphasize the critical role of spatiotemporal variability in shaping meteorological drought patterns across Bangladesh. The dominance of droughts in the northwest and northeast regions highlights the influence of geomorphic features, such as higher elevations and sandy soils in *Char* areas, which exacerbate water scarcity. The support of monsoon rainfall for stocking up water resources accentuates the vulnerability of these regions during years with below-average precipitation, particularly during dry seasons. The seasonal imbalance in rainfall distribution, with significant rainfall concentrated in July and prolonged dry periods during winter months, creates challenges for sustainable water management and agricultural planning (Al Shoumik et al. 2023; Sarkar et al. 2024). Addressing these

vulnerabilities requires integrating seasonal precipitation forecasts, improving irrigation infrastructure, and adopting drought-resilient agricultural practices to mitigate the adverse impacts of meteorological drought in the context of climate variability and change (Alamgir et al. 2015; (Rahman, 2018); Al Mamun et al. 2024).

### 3.4 Seasonal Assessment of Agricultural and Meteorological Drought Using Advanced Indices

The seasonal patterns of agricultural and meteorological droughts in the study area were analyzed using the ADRI, VHI, SPI, and WUE (Fig. 8). The pre-monsoon seasons (January to April) exhibited severe drought conditions, with the VHI and ADRI indicating significant stress in 2006, 2009, 2014, and 2019. The SPI also showed moderate drought during these periods, reflecting the transition from dry to extremely hot conditions with minimal precipitation. Conversely, the post-monsoon seasons (September to December) demonstrated more varied responses. While the VHI and ADRI highlighted favorable conditions in 2012, 2017, and 2021 due to sufficient water availability for winter Boro rice cultivation, the SPI indicated mild drought during this period, as precipitation levels were 64% lower than the monsoon average. The monsoon seasons (May to August) were mostly drought-free due to favorable rainfall and climatic conditions. The correlation between the VHI

**Fig. 8** Time-series comparison of drought dynamics and water use efficiency (WUE) in the study area. Seasonal drought variations are shown through the Vegetation Health Index (a), Standardized Precipitation Index (b), and Agricultural Drought Response Index (c), along with water-use efficiency (d). The pre-monsoon period (January to April) experiences significant drought stress, while the monsoon season generally alleviates drought conditions. In the post-monsoon period (September to December), the SPI indicates mild drought despite sufficient water for crops, and the VHI trends demonstrate agricultural recovery

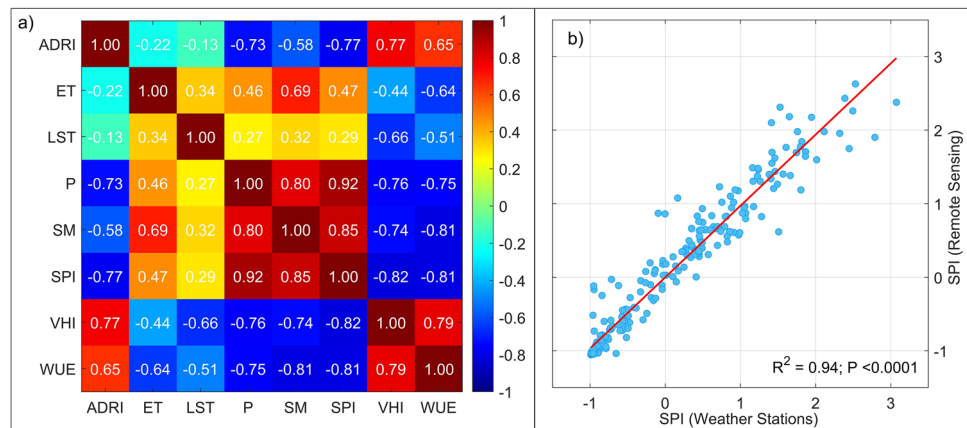
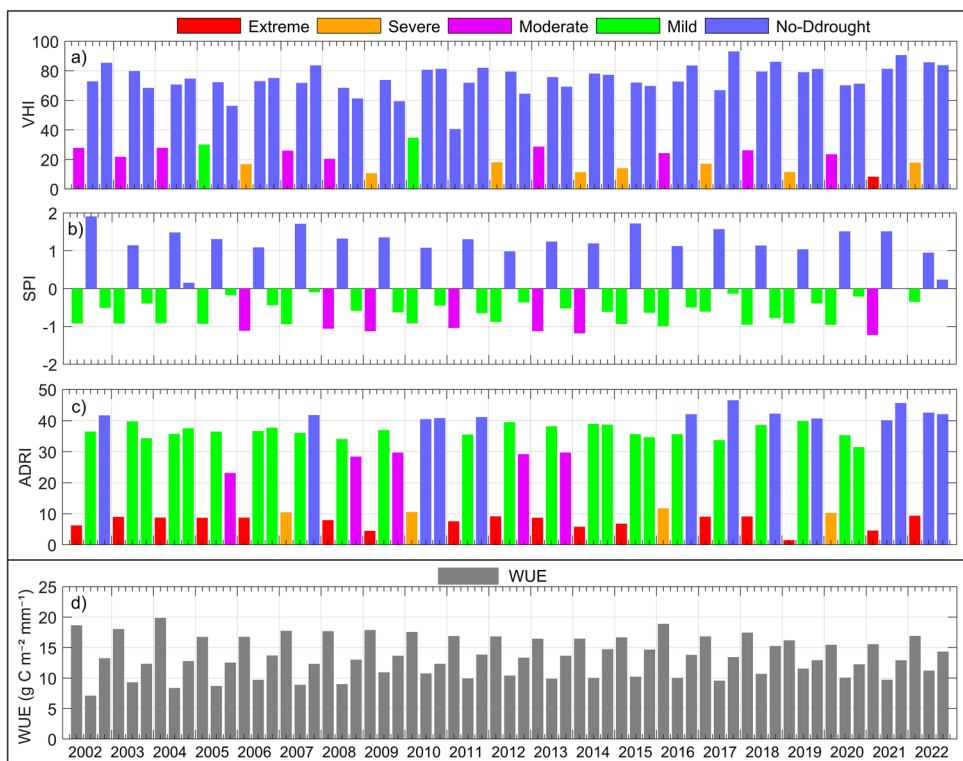


**Fig. 9** (a) Correlation heatmap of climate variables, drought indices, and water balance. LST represents Land Surface Temperature, while the other variables include Soil Moisture (SM), Standardized Precipitation Index (SPI), Vegetation Health Index (VHI), Agricultural Drought Response Index (ADRI), Evapotranspiration (ET), and Water

Use Efficiency (WUE). (b) Relationship between the remotely sensed SPI and the observed SPI (weather station-based) using data from the Bangladesh Meteorological Department (BMD). The analysis reveals a strong correlation, with an  $R^2$  value of 0.94 and a highly significant  $p$ -value ( $< 0.0001$ )

and ADRI ( $R^2 = 0.98$ ,  $p < 0.001$ ) demonstrated consistency in capturing agricultural drought dynamics, while ADRI's NDVI-based approach highlighted the influence of vegetation health on drought assessments.

The variable interaction heatmap (Fig. 9.a) reveals expected and non-intuitive relationships among drought drivers. Strong positive correlations between soil moisture and vegetation health ( $R^2 = 0.85$ ), and between precipitation and vegetation health ( $R^2 = 0.79$ ), affirm that water availability directly supports crop growth. Interestingly, the negative

correlation between precipitation and evapotranspiration ( $R^2 = -0.44$ ) challenges common assumptions. During heavy rainfall, lower temperatures and reduced solar radiation may suppress evapotranspiration, despite water availability. This finding has implications for climate projections where increased rainfall may not equate to increased moisture stress relief, especially if thermal dynamics counteract expected gains.

Another notable result is the negative relationship between vegetation health and water use efficiency (WUE;

$R^2 = -0.81$ ). This suggests that under drought stress, vegetation becomes more water-efficient, possibly as a physiological response to conserve moisture. It also raises questions about the role of plant type, nutrient availability, and management practices in moderating these outcomes—factors that must be integrated into future drought models to enhance prediction accuracy.

The integration of SPI from weather station observations (Fig. 9b) with satellite-derived SPI shows a strong agreement ( $R^2 = 0.94$ ,  $p < 0.0001$ ), confirming the robustness of remote sensing approaches for drought tracking. This strengthens confidence in deploying these tools for early warning systems, particularly in data-scarce regions.

Importantly, the seasonal drought trends identified in this study align with climate change projections for Bangladesh, which predict increased dry season warming, inconsistent rainfall patterns, and longer drought durations. These trends underscore the urgent need for seasonally adaptive and region-specific drought mitigation strategies. Integrating multi-index approaches like SPI, VHI, and ADRI allows for more nuanced monitoring and informed decision-making. Future resilience planning should prioritize improved irrigation infrastructure, adoption of drought-resilient crop varieties, and integration of planning tools to reduce agricultural vulnerability under projected climate stress (Ahmed et al. 2023; Alam et al. 2023; Fattah et al. 2023).

### 3.5 Water-Use Efficiency and Drought Adaptation in Agricultural Systems

WUE was derived from MODIS-based GPP and ET data, revealing an average WUE of  $13.47 \text{ g C m}^{-2} \text{ mm}^{-1}$  over the study period. The highest WUE of  $19.87 \text{ g C m}^{-2} \text{ mm}^{-1}$  occurred during the pre-monsoon period of 2004, while the lowest,  $7.11 \text{ g C m}^{-2} \text{ mm}^{-1}$ , was observed in the monsoon season of 2002. This variability highlights the agricultural system's adaptive response to seasonal water availability. During drought periods, particularly in pre-monsoon seasons, WUE increased as ecosystems optimized their water usage under scarcity (McKee et al. 1993; Srivastava et al. 2024). Significant negative correlations were identified between WUE and drought indices, with  $R^2$  values of 0.68, 0.85, and 0.66 for the VHI, SPI, and ADRI, respectively, suggesting that higher drought severity is accompanied by enhanced water efficiency.

The outcomes demonstrate the critical role of WUE as a measure of agricultural adaptation to water scarcity. During drought conditions, the observed increase in WUE reflects the ecosystem's capacity to optimize water use, mitigating the impacts of reduced water availability on productivity. The strong negative correlations between WUE and drought indices (VHI, SPI, and ADRI) further highlight

this adaptive response, where agricultural systems adjust to intensify water-use efficiency as drought severity increases (Hatfield and Dold 2019; Prodhan et al. 2020; Rahman et al. 2023; Mamun et al. 2024). This relationship underscores the importance of WUE in drought resilience and provides valuable insights for sustainable water management practices.

These results emphasize the need for targeted interventions, such as drought-resistant crops and precision irrigation techniques, to support agricultural systems in maintaining productivity under water-limited conditions. By integrating WUE into drought monitoring and management strategies, policymakers and agricultural stakeholders (small-scale and large-scale farmers) can enhance the resilience of farming practices to the challenges posed by climate variability and water stress (Srivastava et al. 2024; Morepje et al. 2024).

Moreover, the observed WUE dynamics have significant implications for ecosystem productivity and resource sustainability. Higher WUE during dry periods reflects an increased ratio of carbon uptake to water loss, which is essential for maintaining yields in Bangladesh's monsoon-dependent agricultural ecosystems. The balance between GPP and ET—especially during transitional periods—is influenced by both climatic drivers (e.g., solar radiation, temperature) and soil moisture conditions, all of which show clear seasonal variability. During the monsoon, abundant rainfall and radiation promote higher ET and photosynthetic rates, while in winter, reduced solar input and lower temperatures constrain ET and plant activity. Importantly, the interaction between soil moisture, precipitation, and LST reinforces the importance of integrated climate–water–carbon modeling to guide drought adaptation. Soil moisture patterns closely follow precipitation regimes, governing both ET and vegetation stress levels. These seasonal couplings indicate that enhancing WUE through informed irrigation practices and crop selection can significantly mitigate the adverse impacts of climate-induced drought on agriculture.

In summary, the strong responsiveness of WUE to seasonal drought patterns highlights its potential as both an indicator and a tool for adaptation. Embedding WUE into national drought monitoring systems will support farmers and policymakers in developing targeted interventions to improve agricultural resilience, water efficiency, and long-term food security under increasing climate stress (Ahmed et al. 2024; Srivastava et al. 2024; Morepje et al. 2024; Yang et al. 2024; Rambal et al. 2025).

### 3.6 Climatic Drivers on Drought Indices and Assessment

To assess the reliability and consistency of various drought indices and the use of water efficiency, we evaluated their association with the NDVI, a widely accepted proxy for

**Fig. 10** The relationship between Normalized Difference Vegetation Index (NDVI) and various drought indices. Panel (a) illustrates the relationship between NDVI and Agricultural Drought Response Index (ADRI), indicating vegetation response to agricultural drought. Panel (b) shows the connection between NDVI and Vegetation Health Index (VHI), reflecting vegetation health under thermal and moisture stress. Panel (c) presents the association between NDVI and Standardized Precipitation Index (SPI), linking vegetation activity to precipitation anomalies. Panel (d) displays the relationship between NDVI and Water Use Efficiency (WUE), highlighting how efficiently vegetation uses water in relation to greenness

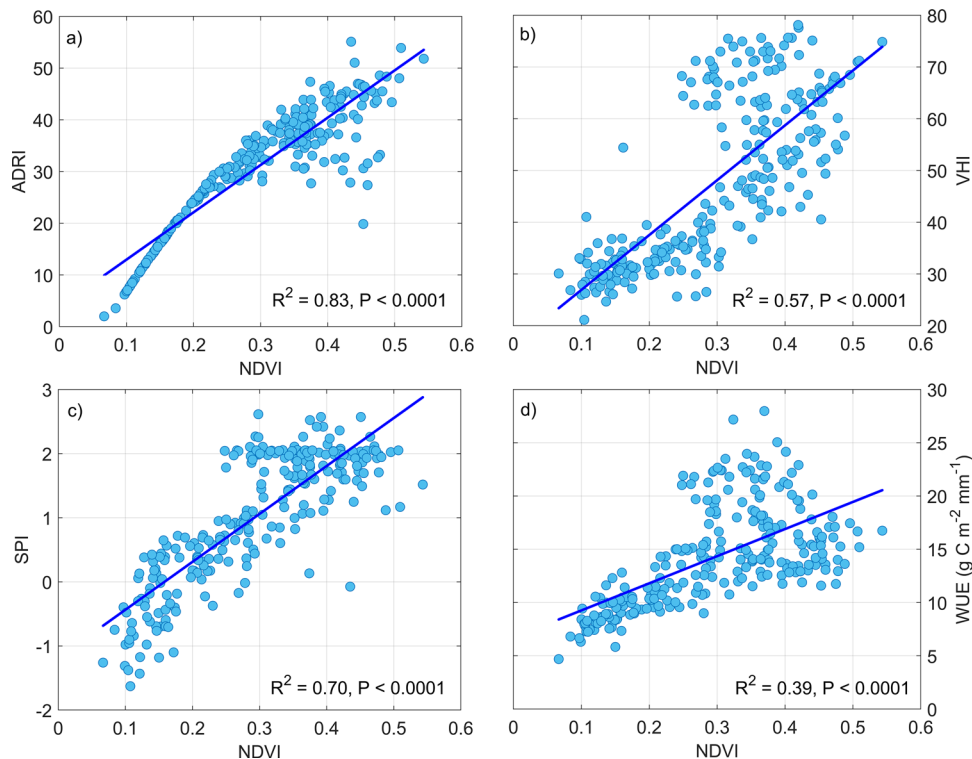


**Table 3** The correlations between the different drought indices and Climatic variables. The strong correlation coefficient was observed with the  $p$ -values of  $<0.0001$ . The key indicators of the multivariable linear regression model include the number of observations (N), error degrees of freedom (DF), root mean square error (RMSE), and correlation coefficient ( $R^2$ ), which quantify the contribution of variance in the dependent variable explained by the independent variables

Index	N	DF	RMSE	$R^2$
VHI	252	248	5.93	0.86
SPI	252	248	0.18	0.97
ADRI	252	248	6.98	0.63

vegetation health and drought stress (Fig. 10). All correlations were statistically significant ( $P < 0.0001$ ), indicating strong and meaningful relationships with vegetation conditions.

Among the indices, the ADRI showed the highest correlation with NDVI ( $R^2 = 0.83$ ), highlighting its strong sensitivity to vegetation stress. The SPI also demonstrated a strong correlation ( $R^2 = 0.70$ ), confirming its effectiveness in capturing precipitation-driven vegetation responses. The VHI showed a moderate correlation ( $R^2 = 0.57$ ), likely influenced by its combined use of thermal and vegetation data.

Water Use Efficiency (WUE), while moderately correlated with NDVI ( $R^2 = 0.39$ ), reflects longer-term ecosystem productivity and physiological adaptation rather than immediate vegetation stress. These results suggest that ADRI and SPI are most suitable for near-real-time monitoring of agricultural drought in regions where vegetation rapidly responds to water availability.

The multivariable linear regression analysis of meteorological variables, including surface temperature, soil moisture, and precipitation, was performed to evaluate their impact on drought conditions over the study period (Table 3). This model captures the relationship between climatic variables and drought indices, incorporating key indicators such as the number of observations (N), degrees of freedom (DF), root mean square error (RMSE), and coefficient of determination ( $R^2$ ), which provide insights into the variance contributed by both dependent and independent variables (Shewhart et al. 2003; Kutner et al. 2004). The results indicate strong correlations between drought indices and climatic variables, with statistically significant low  $p$ -values ( $< 0.0001$ ).

The VHI exhibited a high correlation ( $R^2 = 0.86$ ), underscoring its sensitivity to vegetation health and drought conditions. Approximately 86% of the VHI variance is explained by climatic factors, with a standard error of 5.93 and a highly significant ( $p < 0.0001$ ). Similarly, the SPI demonstrated the highest correlation ( $R^2 = 0.97$ ), reflecting a strong relationship between precipitation and drought severity, with about 97% of the SPI variance explained by climatic conditions. The ADRI showed a moderately significant correlation ( $R^2 = 0.63$ ;  $p < 0.0001$ ), with 63% of its variance attributed to climatic factors and a standard error of 6.98.

Table 4 provides the model results examining associations between drought indices (VHI, SPI, and ADRI) and climatic variables (LST, soil moisture, and precipitation). For the

**Table 4** Multivariable linear regression analysis of drought indices and specific Climatic factors for each drought index (VHI, SPI, and ADRI) and Climatic variable (LST, soil moisture, and precipitation) by statistical indicators including intercept, estimate, standard error, t-statistics, and *p*-value

VHI				
	Estimate	Standard Error	tStat	<i>p</i> Value
Intercept	146.68	4.54	32.28	<0.0001
LST	-3.19	0.17	-18.62	<0.0001
Soil Moisture	-8.71	11.41	-0.76	0.44
Precipitation	0.06	0.001	-14.37	<0.0001
<b>SPI</b>				
	Estimate	Standard Error	tStat	<i>p</i> Value
Intercept	-0.90	0.13	-6.52	<0.0001
LST	-0.004	0.005	-0.76983	0.44
Soil Moisture	-0.19	0.34	-0.55134	0.58
Precipitation	0.005	0.0001	45.53	<0.0001
<b>ADRI</b>				
	Estimate	Standard Error	tStat	<i>p</i> Value
Intercept	25.27	5.35	4.72	<0.0001
LST	0.41	0.20	2.05	0.04
Soil Moisture	48.16	13.44	3.58	0.0004
Precipitation	-0.06	0.004	-13.85	<0.0001

VHI, the intercept was 146.68, with coefficients of -3.19 for LST, -8.71 for soil moisture, and 0.06 for precipitation. The SPI intercepted -0.90, with coefficients of -0.004 for LST, -0.19 for soil moisture, and 0.005 for precipitation. For the ADRI, the intercept was 25.27, with coefficients of 0.41 for LST, 48.16 for soil moisture, and -0.06 for precipitation. The VHI demonstrated a strong negative association with LST (estimate = -3.19, *p* < 0.0001), indicating that higher temperatures contribute to lower vegetation health. A moderate positive association was found between the VHI and precipitation (estimate = 0.06, *p* < 0.0001), suggesting that increased precipitation supports vegetation growth, mitigating drought impacts. Soil moisture, however, showed a non-significant association with the VHI (*p* = 0.44), indicating that other factors may influence vegetation health beyond soil moisture levels. The SPI exhibited a positive correlation with precipitation (estimate = 0.005, *p* < 0.0001), linking higher precipitation with reduced drought severity. Weak associations were found between the SPI and both LST and soil moisture, affirming precipitation's primary role in SPI dynamics. The ADRI displayed moderate associations with LST (estimate = 0.41, *p* = 0.04) and a strong relationship with soil moisture (estimate = 48.16, *p* = 0.0004), suggesting that higher temperatures and soil moisture variations play a role in drought severity. Additionally, the correlation heatmap illustrates the relationships among key environmental factors, including LST, precipitation, soil moisture, water and energy fluxes (ET, WUE), and various drought indices (Fig. 9.a).

The multivariable regression analysis reveals intricate relationships between climatic factors and drought indices, emphasizing the strong explanatory power of the SPI ( $R^2 = 0.97$ ) and VHI ( $R^2 = 0.86$ ) in modeling drought dynamics. These findings highlight the effectiveness of multivariable regression models in capturing drought patterns, offering valuable insights into the primary drivers of drought. This understanding aids in the development of better preparedness and adaptation strategies, ultimately helping to reduce drought impacts on socioeconomic and environmental systems and enhancing resilience in drought-prone areas (Sarkar et al. 2024; Hasan et al. 2024).

The correlation plot (Fig. 9.b) emphasizes a strong agreement between remote sensing-derived SPI and weather station-based SPI, with an  $R^2$  value of 0.94 ( $P < 0.0001$ ), indicating that satellite-based estimates effectively capture precipitation anomalies. This relationship suggests that remote sensing data can reliably substitute in-situ observations, reducing reliance on sparse weather station networks for drought monitoring. However, slight deviations from the regression line may be attributed to localized precipitation variations or sensor limitations in detecting small-scale heterogeneity. Despite these minor discrepancies, the high correlation coefficient reinforces the potential of remote sensing for providing continuous spatial and temporal drought monitoring, positioning it as a valuable tool for regional climate analysis and water resource management.

The regression analysis further demonstrates that precipitation is the dominant factor influencing drought variability, shown by its strong correlation with the SPI and VHI. Surface temperature also plays a significant role in vegetation health, highlighting the importance of adaptive strategies to mitigate the impacts of heat stress on ecosystems. These results underline the value of multivariable models in identifying the primary climatic drivers of drought, supporting the formulation of targeted water management and agricultural resilience strategies (Hussain et al. 2021; Das et al. 2023; Hasan et al. 2024).

## 4 Discussion

### 4.1 The Climatic Condition

The seasonal climate patterns and soil variability in Bangladesh highlight the complex interactions between temperature, precipitation, ET, and soil moisture (Fattah et al., 2023). LST peak during the monsoon transition in April and May, with cooler conditions in December and January, reflecting monsoonal dynamics (Ahmed et al. 2023; Dastour et al. 2025). Precipitation follows a distinct pattern, with alternating wet and dry years, and the monsoon accounts for 67%

**Table 5** Comparative overview of major drought studies in Bangladesh, including the present study, summarizing methods, study periods, and key findings relevant to spatial-temporal drought patterns, seasonal variability, and climate change impacts

Study	Reference	Study Period	Method/ Data Used	Key Findings
Assessment of drought using SPI	Shahid and Behrawan (2008)	1960–2002	SPI/ Rainfall Data	Identified increasing drought frequency in northwest Bangladesh
Spatiotemporal drought analysis	Shahid (2010)	1961–1992	SPI/GIS, Rainfall Records	Spatial variability in drought; western and northern regions are most vulnerable
Meteorological drought pattern	Alamgir et al. (2015)	1961–2010	SPI/ Rainfall Data	Droughts for pre-monsoon in northwest, monsoon in northwest and winter in west.
Hydro-climatological drought analysis	Rahaman et al. (2016)	1964–2013	Trend Analysis/ Climate Data	Trans-boundary water flow limits surface water, triggering drought.
Spatiotemporal drought analysis	Kamruzzaman et al. (2022)	1980–2018	SPI, SPEI/ Rainfall Data	Temperature affect precipitation; drought intensity rises in northwest.
Drought monitoring	Das et al. (2023)	1990–2020	GIS/ NDVI, NDWI, LULC	NDVI effective for agricultural drought; northwest regions are vulnerable
Climate change and drought	Rahman et al. (2023)	1991–2020	Neural Network/ Meteorological Data	Meteorological data and Neural Network predicted seasonal drought susceptibility.
Meteorological drought assessment	Sadiq et al. (2023)	2010–2019	NDVI, NDWI, GIS/ MODIS Data	Spatial variability in drought; western and northern regions are most vulnerable.
Agricultural Droughts	Mamun et al. (2024)	2000–2020	VHI/ NDVI, LST	Northern region, especially in winter, is more drought prone.
Climate Change and Drought linkage	Present Study (Hussain et al., al., 2025))	2002–2022	SPI, VHI, ADRI, WUE/ Satellite and Station climate data	Droughts are becoming more severe with changing climate; monsoon variability key driver for drought resilience.

of the annual rainfall. Years with significant anomalies, like 2014 and 2018 (drier), and 2017 and 2022 (wetter), impact agriculture, water availability, and flooding risks. These findings underscore the importance of adaptive water resource management to cope with climate variability (Rahman 2018; Sarkar et al. 2024).

ET and soil moisture trends further illustrate the region's climatic sensitivity. ET rates peak in October, driven by post-monsoon energy and soil moisture, while they dip in January and February, reflecting seasonal energy constraints. Soil moisture closely tracks precipitation trends, peaking during the monsoon and declining during dry months (Han et al. 2021; Sharma et al. 2022). These patterns emphasize the need for adaptive land and water management strategies to mitigate drought impacts, prevent waterlogging, and optimize irrigation scheduling (Selvaraju, and Baas, 2007); Dey et al. 2017). The findings provide a foundation for designing resilient agricultural practices and water resource management plans, which are critical for maintaining ecosystem stability in the face of climate variability (Iqbal et al. 2025).

## 4.2 Comparative Analysis of Different Drought Dynamics

This study expands upon existing research on drought dynamics in Bangladesh by confirming the seasonal and spatial variability of droughts, particularly in the *Char* and northwestern regions, where pre-monsoon and dry winter conditions contribute to heightened drought risk (Ahmed et al. 2021). Consistent with earlier studies (e.g., Ahmed 2006; Mojid 2020; Islam and Nursey-Bray 2017), our findings validate the role of monsoon variability, limited soil moisture retention, and upstream water regulation in determining regional drought severity. By integrating remote sensing-derived indices such as VHI, SPI, ADRI, and WUE, this study advances previous work by contributing a more spatially detailed and ecologically responsive assessment of drought impacts. Our results not only align with station-based observations but also provide new insights into adaptive ecosystem responses and multi-seasonal drought risks. The comparative analysis presented in Table 5 highlights methodological improvements and supports the integration of satellite-based tools into climate-resilient agriculture ecosystem planning and localized drought monitoring.

Agricultural drought, caused by soil moisture deficits and vegetation stress, is most severe in regions such as *Char* and *Haor*, where poor water retention and dependence on seasonal rainfall exacerbate the impact of droughts. Meteorological drought, driven by rainfall shortages, follows broader climatic trends, with the northwestern and northeastern regions experiencing frequent dry spells due to reduced river discharge. Notably, the Monga region in the

northwest suffers from severe food insecurity during prolonged droughts, exacerbated by upstream water regulation affecting the Teesta and Brahmaputra rivers (Selvaraju and Baas 2007; Aziz et al. 2022). This study found a strong correlation between remotely sensed and weather station-based SPI, with an  $R^2$  value of 0.94 ( $p < 0.0001$ ), confirming the reliability of satellite-based drought monitoring across Bangladesh (Prodhan et al. 2020; Sadiq et al. 2023).

Seasonal drought patterns across Bangladesh reveal critical vulnerabilities, especially during the pre-monsoon period (January–April). This period is marked by extreme water scarcity, high temperatures, and declining soil moisture, particularly in rain-fed agricultural zones (Sultana et al. 2023; Mamun et al. 2024). The northeastern *Haor* wetlands are especially vulnerable to early-season water shortages, disrupting *Boro* rice cultivation. During the monsoon season (May–August), rainfall replenishes water resources and alleviates drought stress, but floodplain areas often face excessive rainfall and flash floods, creating additional challenges for agriculture. In the post-monsoon period (September–December), while initial water availability supports crop growth, declining rainfall leads to localized drought stress, particularly in the sandy, well-drained soils of *Char* lands (Dey et al. 2017; Islam et al. 2020; Sultana et al. 2023; Rahman et al. 2025). These seasonal patterns highlight the need for region-specific water management strategies, including improved irrigation infrastructure, sustainable transboundary water agreements, and strategic reservoir management to better manage seasonal fluctuations and mitigate the effects of drought (Islam et al., 2017).

The analysis emphasizes the significant impact of seasonal patterns on agricultural and meteorological drought dynamics in Bangladesh. The pre-monsoon period stands out as the most vulnerable, with severe drought conditions due to minimal precipitation and high temperatures, severely affecting agricultural ecosystems and water availability (Sultana et al. 2023; Sarkar et al. 2024). On the other hand, the monsoon season plays a crucial role in replenishing developing the drought conditions by water availability and supporting crop growth. However, drought events have also been observed during the monsoon season in India, with studies highlighting evapotranspiration as a key factor, especially across large areas with diverse ecosystems (Kumar et al. 2013). This study identified significant annual findings based on SPI in 2006, 2013, 2014, and 2018, indicating moderate to severe drought conditions (Fig. 7). These results are consistent with previously published studies as summarized in Table 5 (Rahman 2018; Sadiq et al. 2023; Sarkar et al. 2024). However, the post-monsoon period presents a mixed scenario, with sufficient water initially supporting agricultural activities, but declining precipitation leading to mild drought stress, as indicated by the SPI.

Furthermore, WUE plays a critical role in building agricultural resilience. MODIS-based GPP and ET data reveal an average WUE of  $13.47 \text{ g C m}^{-2} \text{ mm}^{-1}$ , with the highest recorded during the pre-monsoon drought of 2004 ( $19.87 \text{ g C m}^{-2} \text{ mm}^{-1}$ ) and the lowest during the monsoon of 2002 ( $7.11 \text{ g C m}^{-2} \text{ mm}^{-1}$ ). Strong negative correlations were found between WUE and drought indices ( $R^2 = 0.68$  for VHI, 0.85 for SPI, and 0.66 for ADRI), showing that as drought severity increases, crops adjust their water use to maintain productivity. Strengthening early warning systems, improving irrigation infrastructure, adopting drought-resistant crops, and implementing adaptive water management strategies are essential for mitigating drought impacts and ensuring long-term food security and climate resilience in Bangladesh (Islam et al., 2017; Sarkar et al. 2024).

The observed patterns—frequent mild droughts interspersed with episodic moderate-to-severe events—are consistent with long-term shifts in temperature and rainfall regimes. Projected climate scenarios for Bangladesh indicate rising average land surface temperatures ( $27.27 \pm 2.3^\circ\text{C}$ ), with summer extremes exceeding  $32.5^\circ\text{C}$ , and a trend toward erratic monsoon behavior, prolonged dry spells, and shifting rainfall distributions. In severe drought years like 2014, total annual rainfall dropped well below the long-term average (2337 mm to 1980 mm), compounding moisture stress due to increased evapotranspiration rates.

These climate-driven changes are particularly harmful to regions like the northwest, where poor water retention exacerbates drought impacts. Declining precipitation and rising heat will likely increase drought frequency, intensity, and duration—placing significant strain on ecosystem services, agricultural productivity, and food security (Ashik-Ur-Rahman et al., 2024; Rahman et al. 2024). These findings emphasize the urgent need for adaptive drought risk management that incorporates both current observations and future climate projections.

### 4.3 Implications for Ecosystem and Resource Management

This study highlights the significant role of seasonal climate patterns and soil variability in shaping Bangladesh's ecosystems and agricultural systems. Climatic factors such as temperature, precipitation, evapotranspiration, and soil moisture show considerable seasonal and inter-annual variations. Peak temperatures occur in April and May, with the monsoon contributing to 67% of annual rainfall, creating marked seasonal imbalances in water availability. Additionally, evapotranspiration rates peak after the monsoon, intensifying pressure on water resources during dry periods (Sultana et al. 2023). Extreme weather events, such as the dry years of 2006, 2014 and 2018 and the wet years of 2017

and 2022, underscore Bangladesh's vulnerability to climate extremes, calling for adaptive, climate-resilient strategies in agriculture and water management (Prodhan et al. 2020; Sadiq et al. 2023).

The strong correlation between soil moisture and precipitation highlights the critical need for adaptive land and water management strategies. Soil moisture levels peak during the monsoon season but decline sharply during the dry months, emphasizing the necessity of efficient irrigation, water conservation, and measures to prevent waterlogging (Prodhan et al. 2020; Sultana et al. 2023). These findings are crucial for shaping national policies that promote resilient agricultural practices and sustainable water management. Although precision agriculture offers an effective approach to optimizing resource use, its adoption remains limited, especially among small- and medium-scale farmers due to technological and financial constraints. At the local and community levels, agricultural officers play a crucial role in mitigating these challenges by guiding farmers in crop selection, irrigation scheduling, and the adoption of drought-resistant practices (Miheretu and Yimer 2017). However, traditional weather station-based drought monitoring remains inadequate at finer spatial scales due to the limited availability of localized meteorological data. This study demonstrates that remote sensing-based tools can address this gap by providing spatially continuous data, enabling more effective decision-making for local small- and medium-scale agricultural practices. Additionally, existing agroecological assessments require updates at finer scales to account for variations in land use and climate dynamics.

While neighboring countries like India have adopted integrated drought monitoring systems (Asrat and Simane 2018; Shah and Mishra 2020), many still rely on broad scale agroecological zoning that lacks the granularity needed for effective local interventions. Bangladesh must move toward finer-resolution agroecological assessments, incorporating both climate variability and land use changes to enable more effective, place-based adaptation. This includes adapting crop calendars, water budgets, and agro-advisory systems to specific micro-regions, particularly those at high risk of seasonal drought intensification.

The integration of remote sensing data with agroecological assessments can provide deeper insights into how local agricultural systems respond to climate variability and drought patterns. Enhancing agroecological zoning at finer spatial resolutions will enable the development of region-specific strategies, ultimately strengthening climate adaptation efforts, promoting sustainable agricultural practices, and preserving critical ecosystems across Bangladesh's diverse landscapes (Nayak et al. 2019).

The findings of this study provide valuable insight for formulating drought-resilient and ecologically informed

policies in Bangladesh. The documented spatial and seasonal variability in drought patterns highlights the urgent need for regionally tailored adaptation strategies, particularly in highly vulnerable areas such as the Char, Haor, and northwestern regions. Policymakers should prioritize investment in localized irrigation systems, scalable early warning tools based on satellite-derived drought indicators, and finer-scale agroecological zoning that incorporates vegetation health, soil moisture, and socioeconomic vulnerability. Integrating high resolution climate data such as LST, NDVI, and WUE into planning frameworks will be essential for promoting sustainable crop planning, resource allocation, and risk reduction. These data-driven strategies not only improve real-time drought monitoring but also support nutritional stability, agricultural sustainability, and ecosystem resilience in the face of growing climate extremes. Most critically, empowering marginal and smallholder farmers through access to climate services, drought-resilient technologies, and informed agricultural extension can reduce their vulnerability to environmental disruptions and contribute to broader economic stability and food security across Bangladesh's climate-sensitive and emerging economy (Nayak et al. 2019; Morepje et al. 2024).

#### 4.4 Limitations

Despite the strengths of this study, several limitations must be acknowledged. While satellite-derived indices provide valuable spatial and temporal coverage for drought monitoring, the coarse resolution of some remote sensing datasets may limit the detection of localized drought events, particularly in heterogeneous landscapes with varying topography, land use, and microclimates. Additionally, issues such as cloud cover, sensor calibration errors, and data discontinuities can introduce uncertainties that affect the precision of drought severity assessments (Kogan, 1990). Another key limitation lies in the sparse distribution and inconsistent temporal coverage of ground-based weather station data in Bangladesh, which can reduce the robustness of satellite data validation. This is particularly problematic in climatically diverse zones, where localized meteorological observations are critical for calibrating remote sensing outputs. Moreover, validation efforts in this study focused primarily on temperature and precipitation; future research should expand this scope to include land surface temperature (LST), NDVI, and other vegetation-based indices, which can suggest deeper insight into ecological responses to drought stress.

To address these limitations, future studies should pursue higher-resolution remote sensing datasets, integrate multi-source data fusion techniques, and strengthen ground validation networks. Enhanced agroecological zoning and

more comprehensive datasets will improve the detection of spatial-temporal drought variability and enable the development of more targeted, climate-resilient resource management strategies designed to regional needs.

## 5 Conclusions

This study provides a comprehensive assessment of agricultural and meteorological drought dynamics in Bangladesh from 2002 to 2022, employing advanced satellite data and analytical techniques. By integrating key drought indices (VHI, SPI, and ADRI) with climatic variables, this research highlights the spatiotemporal evolution of drought severity and its significant impacts on agricultural productivity. The findings reveal that mild-to-moderate drought conditions persisted throughout the study period, with severe events notably concentrated in 2006, 2011, 2013, 2014, and 2016. Vulnerable regions, such as *Char* areas, low-elevated *Haor* and the north-west region were disproportionately affected due to unfavorable soil properties and limited irrigation infrastructure. Additionally, the study reveals that increasing drought severity, driven by climate variability, is closely linked to enhanced WUE as crops adapt to water-limited conditions. These findings highlight the critical role of WUE trends in shaping agricultural resilience and underscore the need to integrate drought and climate change considerations into sustainable water and crop management strategies.

The multivariate regression analysis underscores the critical role of surface temperature, soil moisture, and precipitation in shaping drought patterns, with the SPI and VHI demonstrating high explanatory power ( $R^2=0.97$  and  $R^2=0.86$ , respectively). Seasonal analysis further highlights the importance of considering seasonal rainfall variability in drought preparedness, as dry pre-monsoon periods exacerbate water scarcity while monsoon seasons typically mitigate drought impacts. The integrated assessment method proposed in this study offers a valuable framework for monitoring drought in Bangladesh and developing region-specific mitigation strategies, which can be adapted for use in other regions facing similar climatic and agricultural challenges.

This study encountered challenges in achieving consistent spatial and temporal resolution across satellite data sources, partly due to the limited availability of ground station data for validation. While remote sensing facilitated continuous monitoring of key variables such as soil moisture, rainfall, and temperature, the inherent differences in sensor characteristics and resolution created difficulties in seamlessly integrating the data. Despite these limitations, this study underscores the potential of multisource remote sensing to fill data gaps and complement traditional

ground-based measurements, although further refinement in data calibration and integration methods is necessary to improve accuracy and reliability.

Future research should integrate climate change projections to assess how shifting conditions influence drought severity, frequency, and distribution, providing insights into long-term trends and guiding adaptation strategies. Additionally, enhancing agroecological zoning at finer spatial scales with remote sensing data will improve understanding of land use shifts and their impact on local agricultural systems and drought resilience. Furthermore, combining advanced remote sensing techniques with machine learning models could improve drought prediction and management. This research is crucial for influencing national policies focused on resilient agriculture and sustainable water management. By providing local farmers with expert guidance, they can make informed decisions on crop selection, irrigation, and drought-resistant strategies.

Importantly, integrating satellite-derived drought indices and WUE into national adaptation frameworks can strengthen localized decision-making, empower marginal farmers, and contribute to long-term agricultural sustainability and economic resilience across climate-exposed Bangladesh economy. The study offers valuable insights into climatic drivers and seasonal drought patterns, forming the basis for evidence-based policies, strategic water planning, and sustainable agricultural practices. These findings enable policymakers and researchers to enhance drought assessment models and implement targeted interventions, fostering resilience in Bangladesh and other drought-prone regions globally.

**Acknowledgements** We want to express our sincere gratitude to A. Z. Md. Zahedul Islam from the Bangladesh Space Research and Remote Sensing Organization for his insightful advice on drought dynamics in Bangladesh. Special thanks are extended to S.M. Shahriar Ahmed, Community and Discussion for Environmental Research (CDER, [www.cder-edu.org](http://www.cder-edu.org)) for providing weather station data from the Bangladesh Meteorology Department (BMD). We gratefully acknowledge the data providers for their contributions to this study. Satellite data from the MODIS were sourced from the Goddard Space Flight Center (<https://modis.gsfc.nasa.gov/data/>). Precipitation data from the Tropical Rainfall Measuring Mission (TRMM) and Global Precipitation Measurement (GPM) were obtained from NASA's global precipitation data site (<https://gpm.nasa.gov/data/directory>). Soil moisture data from the Soil Moisture Active Passive (SMAP) mission were downloaded from NASA's Jet Propulsion Laboratory, California Institute of Technology, California, USA (<https://smap.jpl.nasa.gov/data/>). We also extend our thanks to the School of Earth, Environment & Society, McMaster University, Hamilton, Ontario, Canada, for providing the opportunity to use MATLAB (Version 2024b) and ArcGIS Pro (Version 3.2). We also Acknowledge to 'CHINTA Research Bangladesh' for providing the research fund.

**Authors' Contributions** Nur Hussain contributed to the conceptualization, methodology, formal analysis, data curation, original draft preparation, and visualization of the study. He also played a key role in the

validation process alongside other co-authors. Md Saifuzzaman was involved in the validation process and took responsibility for supervising the research. Additionally, he played a significant role in reviewing and editing the manuscript. Mohd. Shamsul Alam contributed to the writing, reviewing, and editing of the manuscript, ensuring the clarity and accuracy of the research. Md Shamim Ahamed participated in the validation process and contributed to the writing, review, and editing of the manuscript. All authors have read and agreed to the published version of the manuscript.

**Funding Information** This research was supported by CHINTA Research Bangladesh (CHINTA Research fund 2024), located at House No: 4, Road No: 3/A, Sector 15, Block E, Uttara, Dhaka 1230, Bangladesh.

**Data Availability** The datasets used and/or analyzed during the current study are available from the corresponding author on reasonable request.

## Declarations

**Competing Interests** The authors declared that they have no competing interests.

## References

ADB (2012). *Addressing Climate Change and Migration in Asia and the Pacific*; The Asian Development Bank (ADB), Manila, Philippines, 2012

Ahamed A, Bolten J, Doyle C, Fayne J (2017) Near Real-Time flood monitoring and impact assessment systems: case study: 2011 flooding in Southeast Asia. *Remote Sensing of Hydrological Extremes*, pp 105–118

Ahmed AU (2006) Bangladesh climate change impacts and vulnerability: A synthesis. Climate Change Cell, Department of Environment. Comprehensive Disaster Management Programme Government of the People's Republic of Bangladesh. [https://www.preventionweb.net/files/574\\_10370.pdf](https://www.preventionweb.net/files/574_10370.pdf)

Ahmed SM, Abdullah HM, Chowdhury TT, Rahman A, Alam MZ (2023) Long-term quantification of pre and post-monsoon surface water area of Bangladesh. *Remote Sens Appl Soc Environ* 32:101069

Ahmed Z, Ambinakudige S, Fosu B (2024) Does integrating climate change projection with agriculture policy improve agricultural adaptation and food security? Evidence from Bangladesh. *Theoret Appl Climatol* 152:187–203

Ahmed Z, Guha GS, Shew AM, Alam GMM (2021) Climate change risk perceptions and agricultural adaptation strategies in vulnerable riverine char Islands of Bangladesh. *Land Use Policy* 102:105232

Alam E, Hridoy AEE, Tusher SMSH, Islam AR, M. T., Islam MK (2023) Climate change in bangladesh: temperature and rainfall climatology of Bangladesh for 1949–2013 and its implication on rice yield. *PLoS ONE* 18(10):e0292668

Alamgir M, Shahid S, Hazarika MK, Nashrullah S, Harun SB, Shamsudin S (2015) Analysis of meteorological drought pattern during different climatic and cropping seasons in Bangladesh. *JAWRA J Am Water Resour Assoc* 51(3):794–806

Al Mamun MA, Sarker MR, Sarker MAR, Roy SK, Nihad SAI, McKenzie AM, Kabir MS (2024) Identification of influential weather parameters and seasonal drought prediction in Bangladesh using machine learning algorithm. *Sci Rep* 14(1):566

Al-Qinna MI, Hammouri NA, Obeidat MM, Ahmad FY (2011) Drought analysis in Jordan under current and future climates. *Clim Change* 106(3):421–440

Al Shoumik BA, Khan MZ, Islam MS (2023) Spatiotemporal characteristics of meteorological and agricultural drought indices and their dynamic relationships during the pre-monsoon season in drought-prone region of Bangladesh. *Environ Challenges* 11:100695

Amalo LF, Hidayat R (2017) Comparison between remote-sensing-based drought indices in East Java. In *IOP Conference Series: Earth and Environmental Science* (Vol. 54, No. 1, p. 012009). IOP Publishing

Amri R, Zribi M, Lili-Chabaane Z, Duchemin B, Gruhier C, Chehbouni A (2011) Analysis of vegetation behavior in a North African semi-arid region, using SPOT-vegetation NDVI data. *Remote Sens* 3(12):2568–2590

Ashik-Ur-Rahman M, Swarnokar SCC, Ahsan SN, Mohibullah M, Mou SI, Gain AK (2024) Farmers' adaptation practices in climate-stressed coastal Bangladesh: a systematic review. *Environ Res Commun*

Asrat P, Simane B (2018) Farmers' perception of climate change and adaptation strategies in the Dabus watershed, North-West Ethiopia. *Ecol Processes* 7(1):1–13

Aziz MA, Hossain AZ, Moniruzzaman M, Ahmed R, Zahan T, Azim S, Rahman NMF (2022) Mapping of agricultural drought in Bangladesh using geographic information system (GIS). *Earth Syst Environ* 6(3):657–667

Baishakhy SD, Islam MA, Kamruzzaman M (2023) Overcoming barriers to adapt rice farming to recurring flash floods in Haor wetlands of Bangladesh. *Heliyon*. <https://doi.org/10.1016/j.heliyon.2023.e14011>

Bhuiyan C, Singh RP, Kogan FN (2006) Monitoring drought dynamics in the Aravalli region (India) using different indices based on ground and remote sensing data. *Int J Appl Earth Obs Geoinf* 8(4):289–302

Bloomfield JP, Marchant BP (2013) Analysis of groundwater drought using a variant of the standardised precipitation index. *Hydrol Earth Syst Sci Discuss* 10(6):7537–7574

Brammer H (1987) Drought in Bangladesh: lessons for planners and administrators. *Disasters* 11(1):21–29

Brammer H (2014) Bangladesh's dynamic coastal regions and sea-level rise. *Clim Risk Manage* 1:51–62

Carlson TN, Arthur ST (2000) The impact of land use—land cover changes due to urbanization on surface microclimate and hydrology: a satellite perspective. *Glob Planet Change* 25(1–2):49–65

Chen S, Zhang L, Zhang Y, Guo M, Liu X (2020) Evaluation of Tropical Rainfall Measuring Mission (TRMM) satellite precipitation products for drought monitoring over the middle and lower reaches of the Yangtze River basin, China. *J Geogr Sci* 30:53–67

Das AC, Shahriar SA, Chowdhury MA, Hossain ML, Mahmud S, Tusuar MK, Salam MA (2023) Assessment of remote sensing-based indices for drought monitoring in the north-western region of Bangladesh. *Heliyon*. <https://doi.org/10.1016/j.heliyon.2023.e13016>

Dastour H, Alam MM, Dewan A, Hassan QK (2025) Evaluating climatic warming and the modulating effects of surface water and regional variables in western Bangladesh. *Results Eng*. <https://doi.org/10.1016/j.rineng.2024.103864>

Dewan TH (2015) Societal impacts and vulnerability to floods in Bangladesh and Nepal. *Weather Clim Extremes* 7:36–42

Dey NC, Saha R, Parvez M, Bala SK, Islam AS, Paul JK, Hossain M (2017) Sustainability of groundwater use for irrigation of dry-season crops in Northwest Bangladesh. *Groundw Sustain Dev* 4:66–77

Domenikiotis C, Spiliotopoulos M, Tsilos E, Dalezios NR (2004) Early cotton production assessment in Greece based on a

combination of the drought vegetation condition index (VCI) and the bhalme and mooley drought index (BMDI). *Int J Remote Sens* 25(23):5373–5388

Du D, Dong B, Zhang R, Cui S, Chen G, Du F (2024) Spatiotemporal dynamics of irrigated cropland water use efficiency and driving factors in Northwest China's Hexi corridor. *Ecol Processes* 13(1):72

Du L, Tian Q, Yu T, Meng Q, Jancso T, Udvardy P, Huang Y (2013) A comprehensive drought monitoring method integrating MODIS and TRMM data. *Int J Appl Earth Obs Geoinf* 23:245–253

Fattah MA, Gupta SD, Farouque MZ, Ghosh B, Morshed SR, Chakraborty T, Rahman MT (2023) Spatiotemporal characterization of relative humidity trends and influence of climatic factors in Bangladesh. *Heliyon*. <https://doi.org/10.1016/j.heliyon.2023.e19991>

Gao BC (1996) NDWI—a normalized difference water index for remote sensing of vegetation liquid water from space. *Remote Sens Environ* 58(3):257–266

Giese L, Baumberger M, Ludwig M, Schneidereit H, Sánchez E, Robroek BJ, Meyer H (2025) Recent trends in moisture conditions across European peatlands. *Remote Sens Appl Soc Environ* 37:101385

Gitelson AA, Kogan F, Zakarin E, Spivak L, Lebed L (1998) Using AVHRR data for quantitative estimation of vegetation conditions: calibration and validation. *Adv Space Res* 22(5):673–676

Gupta N, Mahato PK, Patel J, Omar PJ, Tripathi RP (2022) Understanding trend and its variability of rainfall and temperature over Patna (Bihar). Current directions in water scarcity research, vol 7. Elsevier, pp 533–543

Guria R, Mishra M, da Silva RM, dos Santos CAC, Santos CAG (2025) Multisensor integrated drought severity index (IDSI) for assessing agricultural drought in odisha, India. *Remote Sens Applications: Soc Environ* 37:101399

Guttman NB (1999) Accepting the standardized precipitation index: a calculation algorithm 1. *JAWRA J Am Water Resour Assoc* 35(2):311–322

Gu Y, Hunt E, Wardlow B, Basara JB, Brown JF, Verdin JP (2008) Evaluation of MODIS NDVI and NDWI for vegetation drought monitoring using Oklahoma Mesonet soil moisture data. *Geophys Res Lett*. <https://doi.org/10.1029/2008GL035772>

Han SC, Ghobadi-Far K, Yeo IY, McCullough CM, Lee E, Sauber J (2021) Grace follow-on revealed Bangladesh was flooded early in the 2020 monsoon season due to premature soil saturation. *Proc Natl Acad Sci U S A* 118(47):e2109086118

Harishnaika N, Ahmed SA, Kumar S, Arpitha M (2022) Computation of the spatio-temporal extent of rainfall and long-term meteorological drought assessment using standardized precipitation index over Kolar and Chikkaballapura districts, Karnataka during 1951–2019. *Remote Sens Appl Soc Environ* 27:100768

Hasan I, Mizanur R, Urmee A, Ananta S, Sabuj R, Khan SK, Chat-topadhyay N (2024) Agrometeorological information for climate resilient agriculture in Bangladesh. *Boletín-Organización Meteorológica Mundial* 73(2):41–46

Hatfield JL, Dold C (2019) Water-use efficiency: advances and challenges in a changing climate. *Front Plant Sci* 10:103

Hazaymeh K, Hassan QK (2017) A remote sensing-based agricultural drought indicator and its implementation over a semi-arid region, Jordan. *J Arid Land* 9:319–330

Hosseini M, Saradjian MR (2011) Multi-index-based soil moisture estimation using MODIS images. *Int J Remote Sens* 32(21):6799–6809

Huang J, Zhuo W, Li Y, Huang R, Sedano F, Su W, Zhang X (2020) Comparison of three remotely sensed drought indices for assessing the impact of drought on winter wheat yield. *Int J Digit Earth* 13(4):504–526

Hussain N, Arain MA, Wang S, Parker WC, Elliott KA (2024) Evaluating the effectiveness of different variable retention harvesting treatments on forest carbon uptake using remote sensing. *Remote Sens Appl Soc Environ* 33:101124

Hussain N, Firdaus F, Rizwan M (2021) Remote sensing of photosynthesis, vegetation productivity and climate variability in Bangladesh. Re-envisioning remote sensing applications. CRC, pp 151–168

Hussain N, Islam MN (2020) Hot spot (G i\*) model for forest vulnerability assessment: a remote sensing-based geo-statistical investigation of the Sundarbans mangrove forest, Bangladesh. *Model Earth Syst Environ* 6(4):2141–2151

Hussain N, Khanam R, Khan E (2017) Two and half century's changes of world largest Mangrove forest: a geo-informatics based study on Sundarbans Mangrove forest, Bangladesh, India. *Mod Environ Sci Eng* 3(06):419–423

Hussain T, Hussain N, Tahir M, Raina A, Ikram S, Maqbool S, Duangpan S (2022) Impacts of drought stress on water use efficiency and grain productivity of rice and utilization of genotypic variability to combat climate change. *Agronomy* 12(10):2518

Iqbal MH, Naznin MT, Hossein MZ (2025) Harnessing nature-based solutions for resilient coastal agriculture: A case study of Southwest Bangladesh. *Nature-Based Solutions*, 7, 100209 <https://doi.org/10.1016/j.nbsj.2024.100209>

Islam MS, Roy S, Afrin R, Mia MY (2020) Influence of climate-induced disasters and climatic variability on cropping pattern and crop production in Bangladesh. *Environ Dev Sustain* 22:8679–8701

Islam MT, Nursey-Bray M (2017) Adaptation to climate change in agriculture in Bangladesh: the role of formal institutions. *J Environ Manage* 200:347–358

Islam MT, Shalehin M, Jahan N, Islam MR, Adham AKM (2024) Modeling boro rice water requirements and irrigation schedules in Mymensingh, Bangladesh, under subtropical climate change. *Results Eng* 24:103665

Jahangir Alam ATM, Saadat AHM, Rahman S, M., Rahman S (2014) Spatio-temporal variation of agricultural drought in the Barind region of bangladesh: an application of a Markov chain model. *Irrig Sci* 63(3):383–393

Jiao W, Zhang L, Chang Q, Fu D, Cen Y, Tong Q (2016) Evaluating an enhanced vegetation condition index (VCI) based on VIUPD for drought monitoring in the continental united States. *Remote Sens* 8(3):224

Jolliffe IT and Cadima J (2016) Principal component analysis: a review and recent developments. *Philos Trans R Soc Lond A Math Phys Eng Sci* 374(2065):20150202

Kamruzzaman M, Almazroui M, Salam MA, Mondol MAH, Rahman MM, Deb L, Islam ARMT (2022) Spatiotemporal drought analysis in Bangladesh using the standardized precipitation index (SPI) and standardized precipitation evapotranspiration index (SPEI). *Sci Rep* 12(1):20694

Karim MR, Rahman MA (2015) Drought risk management for increased cereal production in Asian least developed countries. *Weather Clim Extremes* 7:24–35

Kogan FN (1990) Remote sensing of weather impacts on vegetation in non-homogeneous areas. *Int J Remote Sens* 11(8):1405–1419

Kogan FN (1995) Application of vegetation index and brightness temperature for drought detection. *Adv Space Res* 15(11):91–100

Kogan FN (2002) World droughts in the new millennium from AVHRR-based vegetation health indices. *Eos Trans Am Geophys Union* 83(48):557–563

Kohl E, Knox JA (2016) My drought is different from your drought: a case study of the policy implications of multiple ways of knowing drought. *Weather Clim Soc* 8(4):373–388

Kumar KN, Gupta A, Mohan TS, Mishra AK, Ashrit R, Momin IM, Rajeevan M (2024) Unraveling subseasonal drought dynamics in

India: insights from NCMRWF extended range prediction system. *J Hydrometeorol* 25(8):1191–1207

Kumar KN, Rajeevan M, Pai DS, Srivastava AK, Preethi B (2013) On the observed variability of monsoon droughts over India. *Weather Clim Extremes* 1:42–50. <https://doi.org/10.1016/j.wace.2013.07.006>

Kumar V, Chu HJ (2024) Spatiotemporal consistency and inconsistency of meteorological and agricultural drought identification: a case study of India. *Remote Sens Appl Soc Environ* 33:101134

Kutner MH, Nachtsheim C, Neter J, Li W (2004) Applied linear statistical models. McGraw-Hill, New York, NY, USA

Leng P, Li ZL, Duan SB, Gao MF, Huo HY (2017) A practical approach for deriving all-weather soil moisture content using combined satellite and meteorological data. *ISPRS J Photogramm Remote Sens* 131:40–51

Madakumbura GD, Kim H, Utsumi N, Shiozama H, Fischer EM, Seland, ... Oki T (2019) Event-to-event intensification of the hydrologic cycle from 1.5 C to a 2 C warmer world. *Sci Rep* 9(1):3483

Mamun MAA, Alauddin M, Meraj G, Almazroui M, Ehsan MA (2024) Evaluating the spatiotemporal variation of agricultural droughts in Bangladesh using MODIS-based vegetation indices. *Earth Syst Environ* 8(4):997–1010

Mannocchi M (2023) Mainstreaming of Nature-Based solutions for the mitigation of hydro-meteorological hazard: governance analysis of a socio-technical change. <https://doi.org/10.48676/unibo/amsdottorato/11054>

McKee TB, Doesken NJ, Kleist J (1993) The relationship of drought frequency and duration to time scales. In *Proceedings of the 8th Conference on Applied Climatology* (Vol. 17, No. 22, pp. 179–183)

Miheretu BA, Yimer AA (2017) Determinants of farmers' adoption of land management practices in Gelana sub-watershed of Northern highlands of Ethiopia. *Ecol Process* 6:1–11

Mishra AK, Singh VP (2010) A review of drought concepts. *J Hydrol* 391(1–2):202–216

Miyan MA (2015) Droughts in Asian least developed countries: vulnerability and sustainability. *Weather Clim Extremes* 7:8–23

MOF (2010) Bangladesh Economic Review. Ministry of Finance (MOF), Government of Bangladesh, Dhaka, Bangladesh

Mohsenipour M, Shahid S, Chung ES, Wang XJ (2018) Changing pattern of droughts during cropping seasons of Bangladesh. *Water Resour Manage* 32:1555–1568

Mojid MA (2020) Climate change-induced challenges to sustainable development in Bangladesh. In *IOP conference series: earth and environmental science* (Vol. 423, No. 1, p. 012001). IOP Publishing

Mondol MAH, Ara I, Das SC (2017) Meteorological drought index mapping in Bangladesh using standardized precipitation index during 1981–2010. *Adv Meteorol* 2017(1):4642060

Morepje MT, Agholor IA, Sithole MZ, Mgwenya LI, Msweli NS, Thabane VN (2024) An analysis of the acceptance of water management systems among smallholder farmers in Numbi, Mpumalanga Province, South Africa. *Sustainability* 16(5):1952

Morris KR, Sehwaller MR, Wolff DB, Pippitt JL (2007) August A global precipitation mission (GPM) validation network prototype. In *3 Int. Conf. on Radar Meteor*

Nagarajan R (2010) *Drought Assessment*; Springer: New-Delhi, India; ISBN:9789048124992

Nayak AK, Shahid M, Nayak AD, Dhal B, Moharana KC, Mondal B, Pathak H (2019) Assessment of ecosystem services of rice farms in eastern India. *Ecol Process* 8:1–16

Newton IH, Hasan MH, Razzaque S, Roy SK (2024) Assessment of climate-induced rice yield using ordinary least squares (OLS) regression analysis: a case study from coastal context. *Earth Syst Environ* 8(4):1437–1451

Nugraha ASA, Kamal M, Murti SH, Widyatmanti W (2023) Development of the triangle method for drought studies based on remote sensing images: A review. *Remote Sens Applications: Soc Environ* 29:100920

Padrón RS, Gudmundsson L, Decharme B, Ducharne A, Lawrence DM, Mao J, Seneviratne SI (2020) Observed changes in dry-season water availability attributed to human-induced climate change. *Nat Geosci* 13(7):477–481

Prodhan FA, Zhang J, Bai Y, Sharma TPP, Koju UA (2020) Monitoring of drought condition and risk in Bangladesh combined data from satellite and ground meteorological observations. *IEEE Access* 8:93264–93282

Rahaman KM, Ahmed FRS, Nazrul Islam M (2016) Modeling on climate induced drought of north-western region, Bangladesh. *Model Earth Syst Environ* 2:1–21

Rahman HT (2018) *Livelihood vulnerability to Climatic stresses: A study of the Northeastern flood plain communities of Bangladesh*; McGill university. Montreal, QC, Canada

Rahman MM, Chowdhury MMI, Amran A, Malik MIU, Abubakar K, Aina IR, Rahman YA, S. M (2024) Impacts of climate change on food system security and sustainability in Bangladesh. *J Water Clim Change* 15(5):2162–2187

Rahman MM, Tripathi NK, Mozumder C, Kongwarakom S, Virdis SGP (2025) Mapping Boro rice cultivation in Bangladesh using Multi-Temporal MODIS data and phenological approach. *Earth Syst Environ*, 1–19

Rahman M, Tumon MSH, Islam MM, Chen N, Pham QB, Ullah K, Dewan A (2023) Could climate change exacerbate droughts in Bangladesh in the future? *J Hydrol* 625:130096

Rambal S, Cavender-Bares J, Limousin JM, Salmon Y (2025) A multi-scale analysis of drought effects on intrinsic water use efficiency in a mediterranean evergreen oak forest. *Agric For Meteorol* 361:110283

Rayhan M, Afroz R (2024) Evaluating climate models to analyze drought conditions in the Western region of Bangladesh. *Prog Disaster Sci* 23:100356

Sadiq MA, Sarkar SK, Raisa SS (2023) Meteorological drought assessment in Northern Bangladesh: a machine learning-based approach considering remote sensing indices. *Ecol Indic* 157:111233

Saharwardi MS, Kumar P, Dubey AK, Kumari A (2022) Understanding spatiotemporal variability of drought in recent decades and its drivers over identified homogeneous regions of India. *Q J R Meteorol Soc* 148(747):2955–2972

Saharwardi MS, Mahadeo AS, Kumar P (2021) Understanding drought dynamics and variability over Bundelkhand region. *J Earth Syst Sci* 130(3):122

Sarkar SK, Das S, Rudra RR, Ekram KMM, Haydar M, Alam E, Islam ARMT (2024) Delineating the drought vulnerability zones in Bangladesh. *Sci Rep* 14(1):25564

Satoh Y, Shiozama H, Hanasaki N, Pokhrel Y, Boulange JES, Burek P, Yokohata T (2021) A quantitative evaluation of the issue of drought definition: a source of disagreement in future drought assessments. *Environ Res Lett* 16(10):104001

Satyanaarayana B, Mohamad KA, Idris IF, Husain ML, Dahdouh-Guebas F (2011) Assessment of mangrove vegetation based on remote sensing and ground-truth measurements at Tumpat, Kelantan delta, East Coast of Peninsular Malaysia. *Int J Remote Sens* 32(6):1635–1650

Selvaraju R, Baas S (2007) *Climate variability and change: adaptation to drought in Bangladesh: a resource book and training guide* (Vol. 9). Food & Agriculture Org., Rome, Italy. Available online: <https://www.fao.org/4/a1247e/a1247e00.pdf> (accessed on 20 January 2024)

Shah D, Mishra V (2020) Integrated drought index (IDI) for drought monitoring and assessment in India. *Water Resour Res* 56(2):e2019WR026284

Shahid S, Behrawan H (2008) Drought risk assessment in the western part of Bangladesh. *Nat Hazards* 46:391–413

Shahid S, Hazarika MK (2010) Groundwater drought in the Northwestern districts of Bangladesh. *Water Resour Manage* 24:1989–2006

Shah R, Bharadiya N, Manekar V (2015) Drought index computation using standardized precipitation index (SPI) method for Surat district, Gujarat. *Aquat. Procedia* 4:1243–1249

Shamsuddin SD, Alam MS, Roni R (eds) (2020) Climate change: issues & perspectives of South Asia. Shahitya Prakash, Dhaka, Bangladesh

Sharma G, Sharma A, Sinha NK, Sharma OP, Singh A, Pandey AK, Sahu MK (2022) Assessment of long-term climate variability and its impact on the decadal growth of horticultural crops in central India. *Ecol Process* 11(1):61

Shewhart WA, Wilks SS, Balding DJ, Bloomfield P, Cressie NAC, Fisher NI, Johnstone IM, Kadane JB, Ryan LM, Scott DW (2003) Wiley series in probability and statistics. Wiley, New York, USA

Singh RP, Roy S, Kogan F (2003) Vegetation and temperature condition indices from NOAA AVHRR data for drought monitoring over India. *Int J Remote Sens* 24(22):4393–4402

Singh TP, Deshpande M, Das S, Kumbhar V (2022) Drought pattern assessment over Marathwada, India through the development of multivariate advance drought response index. *Int Arch Photogramm Remote Sens Spat Inf Sci* 43:1173–1180

Skofronick-Jackson G, Kirschbaum D, Petersen W, Huffman G, Kidd C, Stocker E, Kakar R (2018) The global precipitation measurement (GPM) mission's scientific achievements and societal contributions: reviewing four years of advanced rain and snow observations. *Q J R Meteorol Soc* 144:27–48

Solomon S, Qin D, Manning M, Chen Z, Marquis M, Averyt KB, Miller HL (2007) Climate change 2007: synthesis report. Contribution of working group I, II and III to the fourth assessment report of the intergovernmental panel on climate change. Summary for Policymakers

Srivastava RK, Purohit S, Alam E, Islam MK (2024) Advancements in soil management: optimizing crop production through interdisciplinary approaches. *J Agric Food Res.* <https://doi.org/10.1016/j.jaf.2024.101528>

Sultana R, Irfanullah HM, Selim SA, Budrudzaman M (2023) Vulnerability and ecosystem-based adaptation in the farming communities of drought-prone Northwest Bangladesh. *Environmental Challenges* 11:100707

Tahasin A, Haydar M, Hossen MS, Sadia H (2024) Drought vulnerability assessment and its impact on crop production and livelihood of people: an empirical analysis of Barind tract. *Helio*. <https://doi.org/10.1016/j.heliyon.2024.e39067>

Talukder B, Saifuzzaman M, VanLoon GW (2015) Sustainability of agricultural systems in the coastal zone of Bangladesh. *Renewable Agric Food Syst* 31(2):148–165

Touma D, Ashfaq M, Nayak MA, Kao SC, Diffenbaugh NS (2015) A multi-model and multi-index evaluation of drought characteristics in the 21st century. *J Hydrol* 526:196–207

United States Geological Survey (2021) Generalized Physiographic Map of Bangladesh (physio8bg): U.S. Geological Survey data release. <https://doi.org/10.5066/P9BP7233>; (Published data: 21-05-2021)

USDA-NRCS (2003) Interpreting the soil conditioning index: A tool for measuring soil organic matter trends. *Soil Quality-Agron. Tech.* US Department of Agriculture, Natural Resources Conservation Service: Washington, DC, USA; [https://www.nrcs.usda.gov/v/sites/default/files/2023-04/nrcs142p2\\_053273.pdf](https://www.nrcs.usda.gov/v/sites/default/files/2023-04/nrcs142p2_053273.pdf) (accessed on 01 July 2024)

Viau AA, Vogt JV, Beaudin I (2000) Comparison of a satellite-based and a precipitation-based drought index. *Can J Remote Sens* 26(6):580–583

Vicente-Serrano SM, Quiring SM, Peña-Gallardo M, Yuan S, Domínguez-Castro F (2020) A review of environmental droughts: increased risk under global warming? *Earth-Sci Rev* 201:102953

Wang S, Huang C, Zhang L, Lin Y, Cen Y, Wu T (2016) Monitoring and assessing the 2012 drought in the Great Plains: analyzing satellite-retrieved solar-induced chlorophyll fluorescence, drought indices, and gross primary production. *Remote Sens* 8(2):61

Wan Z (1999) MODIS land-surface temperature algorithm theoretical basis document (LST ATBD). *Inst Comput Earth Syst Sci Santa Barbara* 75:18

Wilhite DA (2016) Drought as a natural hazard: concepts and definitions. In *Droughts* (pp. 3–18). Routledge, London, UK; pp. 3–18, ISBN 0415168333

Wilhite DA, Sivakumar MV, Pulwarty R (2014) Managing drought risk in a changing climate: the role of national drought policy. *Weather Clim Extremes* 3:4–13

Winkler K, Gessner U, Hochschild V (2017) Identifying droughts affecting agriculture in Africa based on remote sensing time series between 2000–2016: rainfall anomalies and vegetation condition in the context of ENSO. *Remote Sens* 9(8):831

WMO (2012) Standardized precipitation index user guide. World Meteorological Organization (WMO), p 1090

Yang J, Lu X, Liu Z, Tang X, Yu Q, Wang Y (2024) Atmospheric drought dominates changes in global water use efficiency. *Sci Total Environ* 934:173084

Yildiz S, Islam HT, Rashid T, Sadeque A, Shahid S, Kamruzzaman M (2024) Exploring climate change effects on drought patterns in Bangladesh using bias-corrected CMIP6 GCMs. *Earth Syst Environ* 8(1):21–43

Zambrano F, Lillo-Saavedra M, Verbist K, Lagos O (2016) Sixteen years of agricultural drought assessment of the Biobío region in Chile using a 250 m resolution vegetation condition index (VCI). *Remote Sens* 8(6):530

Zeng J, Zhou T, Qu Y, Bento VA, Qi J, Xu Y, Wang Q (2023) An improved global vegetation health index dataset in detecting vegetation drought. *Sci Data* 10(1):338

Zhang A, Jia G (2013) Monitoring meteorological drought in semi-arid regions using multi-sensor microwave remote sensing data. *Remote Sens Environ* 134:12–23

Zhao C, Huang Y, Li Z, Chen M (2018) Drought monitoring of southwestern China using insufficient GRACE data for the long-term mean reference frame under global change. *J Clim* 31(17):6897–6911

**Publisher's Note** Springer Nature remains neutral with regard to jurisdictional claims in published maps and institutional affiliations.

Springer Nature or its licensor (e.g. a society or other partner) holds exclusive rights to this article under a publishing agreement with the author(s) or other rightsholder(s); author self-archiving of the accepted manuscript version of this article is solely governed by the terms of such publishing agreement and applicable law.